Northwest Atlantic Fisheries Organization

Serial No. N7085 **NAFO SCR Doc. 20/037**

SCIENTIFIC COUNCIL MEETING – JUNE 2020

Meteorological, Sea Ice, and Physical Oceanographic Conditions in the Labrador Sea during 2019

Igor Yashayaev, Ingrid Peterson, and Zeliang Wang

Fisheries and Oceans Canada
Ocean and Ecosystem Sciences Division
Bedford Institute of Oceanography
P.O. Box 1006, 1 Challenger Drive
Dartmouth, Nova Scotia B2Y 4A2

Abstract

In the Labrador Sea, wintertime surface heat losses result in the formation of dense waters that play an important role in ventilating the deep ocean and driving the global ocean overturning circulation. In the winters since 2015, the central Labrador Sea (the coldest and freshest North Atlantic basin south of the Greenland-Iceland-Scotland Ridge) experienced above-normal (2016 and 2017) and near-normal (2018 and 2019) surface heat losses. The recent reduction in the seasonal cooling of the Labrador Sea contrasts the situation in 2015 with the highest winter heat loss since 1994. The winter (Dec-Mar) NAO index was moderately positive in 2019. However, atmospheric circulation associated with a low atmospheric pressure anomaly in the Labrador Sea in winter resulted in above-normal air temperatures in the northern and central Labrador Sea. Sea surface temperatures were near-normal in winter and above-normal in spring. Sea ice extent anomalies in winter and spring were generally negative, except for a near-normal winter anomaly on the central Labrador Shelf. With respect to annually averaged temperature anomaly values, in 2018, the upper 100 m layer of the central Labrador Sea was the coldest since 2000. However, between 2018 and 2019, this layer warmed by 0.5°C. The intermediate, 200-2000 m, layer was cooling between 2011 (the layer's warmest year since 1972) and 2018. This cooling trend can be associated with persistent deepening of winter convection over the same time period. The key factor that has contributed to the recurrent deepening of convective mixing in the three winters following the winter of 2015 was not as much air-sea heat exchange as it was the water column preconditioning caused by convective mixing in the previous years. Such multiyear persistence of deepening winter convection (eventually exceeding 2000 m in depth) has resulted in the most voluminous, densest and deepest formation of Labrador Sea Water since 1994. In the winter of 2018-2019 the situation has however changed with winter convection not generally exceeding 1200 m and the intermediate layer warming slightly but enough to reverse the seawater density trend. Between 2018 and 2019, the annual mean intermediate layer density reduced by 0.007 kg/m3. Overall, the changes in the depth of winter convection and intermediate layer properties between these years imply that the effect of the water column preconditioning on winter convection has weakened since 2018. Bedford Institute of Oceanography North Atlantic model simulations suggest that the transport of the Labrador Current decreased between 1995 and 2014, but has since increased slightly. The AMOC from this model demonstrates a general weakening trend since mid-1990s, and continuing weakening in recent years is present in this model hindcast.

Introduction

The Labrador Sea is located between Greenland and the Labrador coast of eastern Canada. Its deep semi-enclosed basin is bounded by the West Greenland and the Newfoundland-Labrador shelves. Cold, low-salinity waters of polar origin circle the Labrador Sea in a counterclockwise current system that includes both the northward flowing West Greenland Current (WGC) on the eastern side and the southward flowing Labrador Current (LC) on the western side (Figure 1). Much warmer and saltier patches of water can be found under the offshore extensions of the WGC and LC. These are variations of the Atlantic Water originating in the low latitudes of the Atlantic Ocean, and following first the North Atlantic Current and then the Gulf Stream. As the Atlantic Water flows into and around the Labrador Sea, following its eastern, northern and eventually western boundaries, it mixes with other masses, progressively cooling and freshening.

Spatial distribution and temporal changes in temperature, salinity, density, dissolved oxygen and other environmental variables in the upper and deep layers of the Labrador Sea respond to a wide range of external and internal oceanic factors. The external factors include exchanges with land, e.g., continental runoff, and atmosphere, e.g., radiation, latent and sensible heat, and momentum fluxes, precipitation, evaporation and exchanges with other substances (such as anthropogenic gases). The internal factors include inflows of warmer and saltier, and colder and fresher waters from the adjacent North Atlantic and Arctic, respectively, and local oceanic processes such as lateral mixing and winter convection. Naturally, the physical, chemical and biological properties throughout the sea (both horizontally and vertically) are subjected to seasonal, interannual and decadal variations in the affecting factors. In addition, instantaneous conditions and process development depend on the cumulative effect of past heat, salt and freshwater gains and respective temperature, salinity and density changes termed as ocean preconditioning (Yashayaev and Loder, 2017).

Since 1990, the Bedford Institute of Oceanography (BIO) has been conducting annual occupations of the oceanographic section Atlantic Repeat 7-West (AR7W). This section spanning the Labrador Sea, (Figure 1, Table 1) was first included as both one-time (A1E) and repeat (AR7W) hydrographic lines in the World Ocean Circulation Experiment (WOCE) array (Lazier et al., 2002; Kieke and Yashayaev, 2015; Yashayaev et al., 2015). Later, the observations collected on the AR7W line became and presently remain an important contribution of Canada to the international Global Climate Observing System (GCOS), the Climate Variability (CLIVAR) component of the World Climate Research Programme (WCRP) and the Global Ocean Ship-based Hydrographic Investigations Program (GO-SHIP).

The annual multidisciplinary survey of AR7W, presently conducted as the core component of the Atlantic Zone Off-shelf Monitoring Program (AZOMP) of Fisheries and Oceans Canada (DFO), has been highlighted in numerous high-impact publications (e.g., Dickson et al., 2002; Curry et al., 2003; Thornalley et al., 2018; Lozier et al., 2019; Frob et al., 2017; Holliday et al., 2020), special journal issues (e.g., Progress in Oceanography, Vol. 73, 3–4, 2007; Progress in Oceanography, Vol. 132, 2015; Yashayaev et al., 2015; Kieke and Yashayaev, 2015), books (e.g., Arctic-Subarctic Ocean Fluxes: Defining the Role of the Northern Seas in Climate, 2008), the Fourth and Fifth Assessment Reports (AR) of the Intergovernmental Panel on Climate Change (IPCC; e.g. Bindoff et al., 2007; Rhein et al., 2013), the International Council for the Exploration of the Sea's (ICES) Reports on Ocean Climate (IROC) and Northwest Atlantic Fisheries Organization (NAFO) reports.

Section AR7W spans approximately 900 km from Misery Point, Labrador, to Cape Desolation, Greenland. Because of heavy sea-ice conditions in some years, the shelf stations cannot always be reached, and hence the shelves are more limited in data coverage than the deep basin and even the slope region. With nearly three decades of annual surveys, the time series now allows an examination of multiyear trends in all key ecosystem variables. Only one year, 2017, was missed in the 30-year long history of the occupations of the AR7W line by BIO. Since 1995, the mid-point date of the survey has occurred between early May and late July, with the earliest dates occurring since 2014, and the latest dates occurring before 2004 (Table 1). For biological variables, the variability in survey date provides information on the seasonal cycles in different regions (Fragoso et al., 2016). For physical variables, the variability in survey date has a significant effect near the surface (0-100 m), but little effect at depths greater than 200 m. In any case, the seasonal cycle has been removed for all depths in this report, in order to provide information on the interannual variability of the physical variables, both near the surface and at depth.

Additionally, the scope of AZOMP activities includes occupations of the Extended Halifax line (XHL, Figure 1), maintaining deep-water oceanographic moorings in the Labrador Sea and on the Scotian Slope and deployments of profiling Argo floats in both regions.

Meteorological Observations

North Atlantic Oscillation (NAO) Index

The NAO is an important teleconnection pattern influencing atmospheric processes in the Labrador Sea (Barnston and Livezey, 1987; Hauser et al., 2015). When the North Atlantic Oscillation (NAO) is in its positive phase, low-pressure anomalies over the Icelandic region and throughout the Arctic combined with high-pressure anomalies across the subtropical Atlantic produce stronger-than-average westerlies across the mid-latitudes. Conditions over the northwestern Atlantic including the Labrador Sea region are colder and drier than average. A negative NAO indicates weakening of both the Icelandic low and Azores high, which decreases the pressure gradient across the North Atlantic resulting in weakening of the westerlies and brings warmer conditions than usual. Both NAO phases are associated with basin-wide changes in the intensity and location of the North Atlantic jet stream and storm track, and in large-scale modulations of the zonal and meridional heat and moisture transport (Hurrell, 1995), resulting in the modification of the temperature and precipitation patterns. Even though the focus of this report is on the past seven decades, we analyze the entire 122-year long record of instrumental NAO observations to relate the recent conditions to the major shifts in the atmospheric situations over the North Atlantic.

NAO index anomalies (relative to the 1981-2010 mean) computed using two versions of the NAO index are shown in Figure 2 (upper panel). The station-based NAO index (green) is the difference in winter (December, January, February, March) sea level atmospheric pressure between the Azores and Iceland (Hurrell et al., 2018). The PC-based NAO index (blue) is associated with the first empirical orthogonal function (EOF) of standardized monthly 500-mb height anomaly fields for the Northern Hemisphere. The spatial pattern of this EOF shows a high over southern Greenland, and a low near the latitude of the Azores.

The wintertime NAO exhibits significant multi-decadal variability (Hurrell, 1995). An upward trend of the NAO index from the 1960s to the 1990s was noted by Visbeck et al. (2001), although since the peak in the 1990s there has been a slight downward trend. Recent studies reveal an atmospheric circulation pattern, complementary to NAO, which becomes more prominent in years of low NAO (Hauser et al., 2015). Further study of this phenomenon will help to improve understanding and forecasting capabilities of atmospheric and oceanic conditions.

In 2010, the NAO index reached a record low (Figure 2, upper panel). In 2011, the NAO index rebounded from the record low but still remained well below the 30-year average (1981-2010). In 2012, however, the NAO index was strongly positive, up to a level comparable to those in early 1990s showing the highest winter index over the last twenty years. There was a significant change in the winter NAO index in 2013, when it became moderately negative. In 2014, the NAO index returned to its high positive phase, slightly lower than the 2012 value, making it the second highest in the last twenty years. In 2015 there was another high NAO event, the largest positive NAO magnitude in the 122-year long instrumental record. In 2019, both the station-based NAO anomaly (green) and the PC-based NAO anomaly (blue) were moderately positive, and have decreased from the extremely high values observed in 2015.

Figure 2 also shows a map of sea level pressure (SLP) anomalies in winter 2019 (December, January, February, March) over the North Atlantic relative to the 1981-2010 mean. A low pressure anomaly can be seen in the Labrador Sea region. This pattern would be associated with stronger-than-normal southerly winds on the eastern side of the Labrador Sea, and northerly winds on the western side.

Air Temperatures

The air temperature data used are from the NCEP Reanalysis dataset, provided by the NOAA/OAR/ESRL PSD, Boulder, Colorado, USA, from their Web site at https://www.esrl.noaa.gov/psd/. The NCEP Reanalysis is a joint project between the National Centers for Environmental Prediction (NCEP) and the National Center for Atmospheric Research (NCAR). The goal of this joint effort is to produce a new Surface Air Temperature and Sea Surface analysis using historical data (1948 onwards) and to produce analyses of the current atmospheric state (Kalnay et al., 1996).

Time series plots of winter and spring air temperature anomalies in the Labrador Basin (55-60°N, 50.0-52.5°W) are shown in Figure 3, and winter and spring maps of surface air temperature anomalies in 2019 from the NCEP Reanalysis are shown in Figure 4. In the winter map, a high positive anomaly can be seen in the northern Labrador Sea, consistent with the low SLP anomaly noted in the previous section.

Air-Sea Heat Flux

The cumulative air-sea heat flux integrated over individual-year cooling seasons (cumulative winter surface heat flux/loss in Figures 3 and 9) was computed using 6-hourly heat flux and daily-mean radiation data obtained from the U.S. National Centers for Environmental Prediction (NCEP) Reanalysis (Kalnay et al., 1996). The two available versions of NCEP Reanalysis products, R1 and R2, are jointly used to provide the most extensive up-to-date data coverage.

The total or cumulative surface heat loss incurred in a cooling season was estimated by integrating the net surface heat flux over the Labrador Basin from start to end of the cooling period. The net heat flux values used in this integration were computed as a sum of incoming and outgoing shortwave and longwave radiative, and latent and sensible turbulent heat flux components extracted for the region of interest from the NCEP/NCAR Reanalysis fields. The start and end points of each cooling cycle were associated with the net flux reversals in fall and spring (Yashayaev and Loder, 2009).

The highest annual heat losses during 1974-2018 were achieved in 1993 and 2015. Since 1998, the top six cumulative surface heat losses have occurred in 2008, 2012, 2014, 2015, 2016 and 2017.

Remotely-Sensed Sea Surface Temperature (SST)

The sea surface temperature data used are from the NOAA Optimum Interpolation (OI) Sea Surface Temperature (SST) V2. NOAA_OI_SST_V2 dataset provided by the NOAA/OAR/ESRL PSD, Boulder, Colorado, USA, from their Web site at https://www.esrl.noaa.gov/psd/. The OISST analysis is constructed by combining observations from satellites, ships, and buoys on a regular global grid, and interpolating to fill in gaps.

Time series plots of winter and spring sea surface temperature anomalies in the Labrador Basin (55-60°N, 50.0-52.5°W) are shown in Figure 3. Winter and spring maps of sea surface temperature anomalies (Figure 5) show positive anomalies in the northern Labrador Sea, especially in the spring, similar to the air temperature anomalies.

Sea Ice Observations

Sea ice concentrations derived from satellite passive microwave data since late 1978 are obtained from the U.S. National Snow and Ice Data Center. These data were used instead of Canadian Ice Service data because they extend farther east, so that they cover the Greenland shelf (comparisons show that the anomalies computed from each dataset for the same area agree very closely).

Monthly sea ice concentration data are used for 1978-2018 (Cavalieri et al., 1996, Fetterer et al., 2002) and daily real-time data are used for 2019 (Meier et al., 2017). Ice extent is defined as the area in which ice concentration is at least 15%, and is computed for three latitude bands in the Labrador Sea region: 63-68°N (Davis Strait), 58-63°N (Northern Labrador Sea), and 53-58°N (Labrador Shelf).

Winter and spring time series of sea ice extent anomalies for these three regions are shown in Figure 6. Winter and spring ice extent anomalies in 2019 are negative for all regions, except the winter anomaly for the Labrador shelf, which was near-normal.

Figure 7 shows monthly maps of sea ice concentration anomalies (top panel) and extent (bottom panel) in January to March 2019, using data from the US National Snow and Ice Data Center. The magenta lines in the lower panel show the median limit of ice extent. In the northern Labrador Sea, negative ice concentration anomalies can be seen, and the ice extent is lower than normal, in agreement with winter air temperature and sea surface temperature anomalies.

Ocean Temperatures and Salinities

Shipboard Observations

Since 2004, the AR7W survey has been carried out mostly in May with at least 30 conductivity-temperature-depth (CTD, although a broader range of sensors than these three are used routinely on every AZOMP mission) and water sampling (e.g., for dissolved oxygen, nutrients, transient tracer) stations occupied between Labrador and Greenland. The pressure, temperature, conductivity, salinity, and dissolved oxygen data sets have been quality controlled and calibrated to meet WOCE standards, using water sample (e.g., Autosal salinity and Winkler titration), SBE35 temperature recorder and laboratory calibration data. Argo float temperature and salinity profiles, available since 2002, have been quality controlled through comparisons with vessel CTD and water sample data and comparisons between floats, and by performing critical analyses of spatial and temporal deviations. The historical and other recent data have also been quality controlled and processed through similar critical analyses (see Yashayaev and Seidov, 2015, for a summary of the data editing and processing approaches used here as well).

The AZOMP and past BIO Labrador Sea data are enhanced and expanded by adding publically available observed-level temperature and salinity data archived by other programs and national and international data centers (e.g., Kieke and Yashayaev, 2015).

Argo Profiling Float Data

Argo is an international network of profiling floats collecting high-quality temperature and salinity profiles from the upper 2000 m of the ice-free global ocean, and through float displacements, currents from intermediate depths. For most of a typical 10-day cycle a battery-powered autonomous float freely drifts at a "parking depth" of usually 1000 m, where its position is stabilized through buoyancy adjustment. Once the float is released from its parking depth, it descents to approximately 2000 m and then ascents to the surface, while profiling temperature, salinity and other variables, if additional sensors are installed. When the surface is reached, the acquired data are transmitted, and the float sinks back to its parking depth. Since 2002, the near real-time temperature and salinity Argo float data collectively draw a large-scale picture of the oceanographic structure and circulation of the Labrador Sea. The array is typically used to reconstruct the seasonal and interannual variability of the physical characteristics and dissolved oxygen in the upper 2000 m water column. The value of the Argo floats is even more significant in winter, when they serve as the only means of providing information about real-time development of winter convection, and when there are no shipboard measurements available.

Overall, the network of profiling Argo floats provided temperature and salinity data to 2000 m used for monitoring of year-round variability of the oceanographic conditions in the Labrador Sea. However, the number of the floats within the Labrador Sea during 2019 was just marginally sufficient to resolve sub-monthly variability.

Synthesis of Multiplatform Data Sets

Temperature and salinity data in the Labrador Sea from various sources are compiled and seasonally adjusted to provide individual time series. Our primary data sources include *(i)* full-depth temperature, salinity, and dissolved oxygen profiles collected on the AR7W line across the Labrador Sea that has been occupied by BIO in support of the WOCE, CLIVAR and other international and departmental ocean climate monitoring and research programs since 1990, *(ii)* water sample and discrete temperature data used to calibrate the instrument sensors, *(iii)* temperature and salinity profiles over the upper 2000 m in the Labrador Sea region from the International Argo float program, *(iv)* publically available observed-level temperature and salinity data from other programs and national and international data centers (e.g., Kieke and Yashayaev, 2015), and *(v)* a near-bottom moored temperature time series from a long-term mooring maintained by the BIO on the Labrador Slope.

The main data additions to the previous years are observations from Argo floats up to March 2020 and DFO's annual CTD survey of the AR7W line across the Labrador Sea in June 2019 (Figure 1).

Following Yashayaev and Loder (2009, 2016 and 2017), but now including all available Argo and ship-based survey data to March 2019, time-depth series of spatially averaged potential temperature, salinity, and

potential density with weekly-to-monthly (dependent on Argo and ship survey data coverage) resolution have been computed for an area of ~60,000 km^2 in the central Labrador Sea.

For each depth level included in a chosen depth layer, a time series has been compiled with all individual CTD, water sample and Argo measurement (profiles) of an analyzed variable within the central Labrador Sea. The measurements have been corrected, depth by depth, for seasonality (wherever applicable) by using an iterative procedure obtaining a harmonic representation of the seasonal cycle and removing data outliers. The resulting series have been low-pass-filtered, and the filtered values have been averaged annually to obtain the annual variable values since 1987.

Further, to place the recent variability in a historical context, we use annual time series of temperature, salinity, and density averaged over the 15-100 and 200-2000 m vertical intervals in the central Labrador Sea back to 1948 as long-term indices of these variables over its upper and intermediate-depth waters. These were derived from time series for selected depths like those discussed above and previously reported.

Winter Convection and Hydrographic Conditions in the Central Labrador Sea

Long-term Changes in Key Water Masses

Multidecadal time-depth distributions of annual temperature, salinity and density (with respect to 1000 dbar pressure) values in the central Labrador Sea since 1950 at depths of 200-3500 m are shown in Figure 8. A combination of averaging on constant density and constant pressure surfaces or levels was used in the computational procedure to achieve best representation of annual seawater characteristics. The intermediate, deep and abyssal or bottom water masses found in the Labrador Sea are LSW, Northeast Atlantic Deep Water (NEADW, 2500-3000 m), and Denmark Strait Overflow Water (DSOW, defined as a 200 m thick bottommost layer at the water depths exceeding 3000 m). Similarly to DSOW, NEADW is also derived from the Iceland-Scotland Overflow Water, but undergoes a longer and more substantial mixing, transformation and modification along its path (Yashayaev and Dickson, 2008).

While the temporal changes within NEADW are comparably slow, typically spanning a few decades, and appear to be vertically-uniform (note how NEADW salinity changed 1975 to 2001 to present in Figure 8), both LSW and DSOW exhibit strong variations on decadal and shorter time scales. Recurring warm and saline, and cold and fresh events spread in the upper 2000 m layer mainly occupied by LSW. A period characterized by warming and salinification of this layer that started in the mid-1960s and ended in the early or mid-1970s was followed by a period with opposite trends in temperature and salinity signified by cooling and freshening of LSW culminated in the late 1980s to mid-1990s. This period was characterized by deep winter convection that filled the upper 2000-2500 m layer of the Labrador Sea with cold, dense and relatively fresh water. Milder winters in the early 2000s produced more limited amounts of LSW, which have gradually become warmer, saltier, and less dense than in the previous decade (Yashayaev, 2007).

Time series plots of annual and spring (April-June) mean temperature and salinity values averaged over the 15-100 m and 200-2000 m depth ranges are presented in Figure 9. Both upper, 15-100 m, and deeper, 200-2000 m, layers have been cooling since 2010. However, the freshening trend seen in the newly-formed or newly-ventilated LSW between 2011 and 2016, reversed in 2016, making the LSW formed in the winter of 2018 the densest since the mid-1990s.

In over 90 years of direct oceanographic observations (Figures 8 and 9, earlier years are not included), the intermediate, 200-2000 m, layer of the Labrador Sea experience two periods of sustained warming. The layer's first anomalously warm saline state was reached in the early 1970. The cooling trend that followed this warm event continued until reaching the record minimum in 1994. The intermediate layer was steadily warming after 1994 until it reached the second record warm peak in 2011. Similarly to the warming episode that ended in the early 1970s, the recent warm state did not last very long either. The cooling of the intermediate layer that followed was a direct result of persistently deepening convection during the winters from 2012 through 2018.

The cooling trends of the upper and intermediate layers reversed in 2019 as the amount of heat transferred from the ocean to the atmosphere in the winter of 2019 was the lowest since 2013. The recent warming of the upper and intermediate layers of the Labrador Sea concurs with the reduced heat loss and shallowed convection in the winter of 2019.

Also shown in Figure 9, are the winter NAO and cumulative winter surface heat flux (because the ocean loses heat through each cooling season, this metric can also be regarded as cumulative heat loss). Their low-pass filtered values (centered on the last year of the filter window) represent the combined effect of recent surface heat losses and water column preconditioning in previous years.

Recent Seasonal and Interannual Variability in the Upper 2000 m

Time-depth distributions of temperature, salinity and density (with respect to 1000 dbar pressure) at depths of 0-2000 m since 2002 (when Argo floats became widespread) are presented in Figure 10. The positive temperature and negative density trends established in the top 1000 m of the sea following the cessation of extreme convection in the mid-1990s were repeatedly interrupted by moderately deep convection in the winters of 1999-2000, 2002 (Figure 8), 2008 and 2012 (Figures 8 and 10). These particularly long temperature and density trends kept reestablishing themselves after each interruption, resuming nearly the same directions and rates they had before the interruption. However despite their multiyear persistence, the aforementioned trends reversed their directions to sustained cooling and density increase in the winter of 2014, when deep convection reaching to 1500 m of depth and below spanned a considerable part of the Labrador Basin. Deep convection has deepened progressively over the five consecutive winters – 2014 through 2018. During this period, each convective development produced a colder denser and deeper LSW than the preceding event. As result, the convectively formed water mass, LSW, was getting colder and denser as convection deepened between 2014 and 2018, inclusively. Overall, the progressive cooling of the top 2000 m, and deep and intense winter mixing during the five consecutive winters of 2014 through 2018 have interrupted the general warming and stratification-building trend that has persisted in the intermediate waters of the Labrador Sea since the mid-1990s.

The deep convection event of 2008 is evident in both the temperature and salinity fields. The depth of shallower convection in 2009 was partly reduced because of massive surface freshening in the preceding summer and fall. The conditions in the winter of 2011 were similar to those in the preceding winter with very limited convection (mixed layer depths did not exceed 800 m). Then, in the winter of 2012, convection reached the depths of ~1400 m, which is clearly present in temperature and salinity profiles acquired by both Argo floats and ship survey. Salinity in the top 200 m in 2012 was the lowest since 2003, particularly in the top 50 m. Convection also occurred in the winter of 2013, but it was not as deep as in the previous year, and was mostly limited to the top 1000 m. The situation changed quite significantly in the winter of 2014. Wintertime cooling triggered convective mixing, homogenizing the top 1600 m (and probably even deeper) layer in the central Labrador Sea. Winter convection progressed over the following four years reaching deeper and making the top 2000 m layer colder and denser with every cooling cycle. In the last of these winters, convection reached and exceeded the depth of 2000 m. These persistent trends in temperature (negative), density (positive) and convection depth (positive), spanning 2011-2018 (Figures 8-10), were caused by a multiyear recurrence of relatively strong, but not necessarily extreme, winter cooling, typically coinciding with moderate-to-high positive NAO. The multiyear cooling led to convective preconditioning of the water column in such a way that winter convection continued to deepen even in reduced winter cooling situation. The winter of 2018 has set a good and presently last example of how a preconditioning of a deep basin reservoir in preceding years may affect convection in a current year, further supporting the hypothesis by Yashayaev and Loder (2017). As in the previous two winters, in the winter of 2018, the subpolar North Atlantic basins lost considerably lesser amounts of heat to surface cooling than in the winter of 2015 (the latter demonstrated the highest cumulative surface heat loss in more than two decades). With the exception of the last winter on record (2019), the cumulative 2018 winter heat loss was also the lowest in the Labrador Sea since the winter of 2014. However, despite the continual reduction in winter cooling, the steady increase in the depth of winter convection since 2015 has resulted in the development of the most significant, in terms of volume, depth and density, class of LSW since 1994.

The cumulative 2019 winter heat loss was only slightly less in magnitude than in the previous winter. Yet, unlike the five preceding cases, the last winter brought a rather weak convection setting a limit to the preconditioning endorsement/enhancement of current-year winter convection discussed in our report earlier.

The persistence in deep convective mixing contributing to the massive LSW development in the recent years and the recent cessation of deep convection are effectively shown in the temporal progression of cascading

vertical temperature, salinity and density profiles (Figure 10) as the cold dense water reaches deeper and deeper with time, and then, in 2019 the trend reverses. Each of the freshly-made deepened and densified LSW vintages was in part preserved in the deep basin until the next winter. This figure illustrates the essence of water column preconditioning by winter convection – sustaining or "memorizing" the previous year conditions throughout the intermediate depths at the convection site same as in the previous report. Yet the added year enriches the progression showing a reversal in positive development in winter mixing.

In addition to surface heat flux, another factor that could potentially change convection is surface freshening due to accelerated melting of the Greenland Ice Sheet. However, a recent study by Dukhovskoy et al. (2019) indicates that the effect of the Greenland freshwater flux anomaly brought by the observed acceleration of Greenland Ice Sheet melt is not sufficient to fully explain the present changes in water column salinity and convective activity. In fact, there is no significant negative trend present in surface salinity in the Labrador Basin in the last decade.

Winter Convection Highlights

The sub-monthly temperature, salinity and density data (Figure 10, 2002-2020 with effective temporal resolution of 5-10 days) show that the winter mixed layer and hence convection in the central Labrador Sea reached and even exceeded 2000 m in March of 2018, ending the sustained positive trend in convection depth spanning the winters of 2012 and 2018 except for 2013. The last three winters in this sequence have demonstrated that certain extreme properties, such as low temperature, weak vertical stability and weak overall stratification, imposed on the water column by a stronger-than-usual convective mixing in the previous years, may assist further development of deep convection. In order to reveal and diagnose long-term water-column preconditioning situations such as the one presented here, continuous year-round measurements of temperature and salinity measurements are required. For example, the recent successive deepening of winter mixing (Figure 10) appears as a significant feature in longer-term reconstructions (Figures 8 and 9), yet its true origin and vertical and temporal developments can only be unambiguously mapped with higher-resolution data.

Despite comparable surface heat losses, convection in the winter of 2019 was much shallower than in the winter of 2018. This negative change in the convection depth (positively) adds to our understanding of the recurrent nature of deep convection. It shows when the past-winter preconditioning of the water column loses its significance for development of convection in present and future winters. Indeed, while convection continued to exceed 1500 m and even deepen over the three years first after the surface heat losses started to decline (since the winter of 2015), it happened only on the fourth year when the intensity and depth of winter convection picked the trend in the surface heat loss. It was not the first time when a deep-water preconditioning had a prolonged effect on convection in the Labrador Sea. A similar situation was observed in the 1987-1996 time period. Despite a decline in atmospheric forcing from the previous winter, the Labrador Sea experienced deep convection (>2000 m) in the winter of 1995, whereas there was no deep convection observed in the same basin in the following winter (1996).

Distance-depth plots of temperature, salinity, density and oxygen from the survey data in 1994, 2011, 2012, 2015, 2018 and 2019 are presented in Figures 11-14. An extensive reservoir filled with a newly ventilated, 2000 m deep, cold, dense, fresh, atmospheric gas loaded vintage of LSW is clearly evident in the AR7W seawater property section based on the 2018 May shipboard CTD data. The 2018 vintage of LSW is associated with low temperature (< 3.3°C) and low salinity (< 34.86) between 1000 and 2000 m. The winter convection in the recent time period, 2015-2018, especially in the winter of 2018, is arguably the deepest since the record-deep cooling that reached 2400 m in the winter of 1994. The present LSW year class is one of the largest ever observed outside of the early 1990s.

The sections plots (Figures 11-14) further confirm that winter convection has lost its strength in the winter of 2019, reaching the depth of about 1400 m in the western part of the Labrador Basin, and only about 1000 m in the central and eastern parts, still affecting the distributions of freshwater (salinity) and gases (dissolved oxygen) across the Labrador Sea, but not in the deep intermediate layer as in the previous years.

Numerical Model Results

In this report, an ocean model hindcast from the Bedford Institute of Oceanography North Atlantic Model (BNAM) is used to calculate the variations of the Labrador Current, and the variations of its two branches as well (details in the section of Results and Discussion). The BNAM is based on the NEMO 2.3 (Nucleus for European Modelling of the Ocean) model. It includes an ocean component OPA and a sea ice module LIM (Louvain-la-Neuve Sea Ice Model). The barotropic transport is used to represent the strength of the current. The hindcast period is from 1990 to 2018. This portion of our report is intended to demonstrate changes of the currents, and their potential representation of the AMOC.

The BNAM model domain was selected to include the North Atlantic Ocean (7ºN – 75ºN and 100ºW – 25ºE) with a nominal resolution of 1/12º. The model has a maximum of 50 levels in the vertical, with level thickness increasing from 1 m at the surface to 200 m at a depth of 1250 m and reaching the maximum value of 460 m at the bottom of the deep basins. The maximum depth represented in the model is 5730 m.

Open boundary data are from the GLORYS reanalysis product (Global Ocean ReanalYses and Simulations). The model surface forcing is taken from a combination of CORE (Coordinated Ocean-ice Reference Experiments) and NCEP/NCAR reanalysis forcing. Model forcing variables include air temperature, wind velocities and humidity; daily short- and long-wave radiation, and total precipitation (rain plus snow). No surface restoring to sea surface temperature is applied. However, the model's sea surface salinity is restored to its monthly climatology with a 60-day restoring time scale.

The model was spun-up for 10 years using the CORE normal year forcing. The 10-year spin-up simulation is initialized with a January climatology of temperature and salinity (T-S). The T-S climatology combines the Polar Science Center Hydrographic Climatology (PHC2.1) at high latitudes with the T-S climatology of WOA5 at middle and low latitudes.

For the purposes of the present report the transports were calculated based on modelled flows through the western segment of the AR7W transect.

Variations of the Labrador Current

The variations of the Labrador Current (LC) can be seen as an indicator for the changes in the subpolar North Atlantic circulation, which region plays an important role in the global climate due to the winter convection event in the Labrador Sea. The variations of the LC are often connected to the variations of the AMOC. Here we present the variations of barotropic transports of the LC from an eddy resolving model developed at Bedford Institute of Oceanography (BNAM, e.g., Brickman et al., 2016; Wang et al., 2016; Brickman et al., 2018; Wang et al., 2018).

An EOF analysis of the model output by Wang et al. (2016) presented in Figure 15 suggests that the variability in the Labrador Current can be partitioned into a western Labrador Current (WLC; from the 300-2500 m isobaths), and an eastern Labrador Current (ELC; from the 2500-3300 m isobaths). Following the definition of the WLC and ELC, we calculated the transports of ELC and WLC, and also those of the LC (the summation of the ECL and WLC).

Figure 16 shows the transport anomalies for the LC, ELC and WLC. The WLC in 2019 was marginally weaker than in 2017, about 2 Sv above the 1990-2019 mean, as it has been since 2001.

A declining trend of the ELC began in 1996, coinciding with a significant drop in the winter NAO index in the same year. The trend reversed in 2014, and the ELC was ~4 Sv stronger in 2019 than in 2018, and it became 1 Sv above the 1990-2019 average. Wang et al. (2016) suggested that the ELC is an indicator for the changes in the AMOC, which would imply a possible significant weakening followed by a strengthening of the AMOC since 2014 based on the BNAM hindcast.

Variations of the AMOC

Wang et al. [2019] investigated the variability of the AMOC from the BNAM solution, and they applied the EOF analysis approach to the AMOC for the whole North Atlantic Ocean. Their study proposed the AMOC PC1 as the AMOC index. The AMOC PC1 was found to be representative of the general low frequency changes of the AMOC, and a general weakening trend was found in the 1990-2015 period. The AMOC PC2 represented the

wind-driven Ekman transport portion of the AMOC, which has high frequency variability and has no obvious trend.

The AMOC in this report was the AMOC in depth space. Figure 17 time-latitude plots of the variations of the AMOC in depth and density spaces from 10°N to 60°N using the monthly mean output from 1990 to 2019. A general weakening tendency can be seen in Figure 18. Following the approach in Wang et al. [2019], we applied the EOF approach to the annual mean (de-seasoned) AMOC to compute the EOF patterns and their associated PCs. The EOF1 represents 75% of the total variance, and the EOF2 represents 11%. The EOF patterns are consistent with those in Wang et al. [2019]. The AMOC PC1 clearly shows the continuing weakening trend after 2015. No clear trend is shown in the Ekman portion of the AMOC shown in the AMOC PC2. The Labrador Current has been strengthening in recent years as shown above, and the AMOC solution from BNAM still presents the existing weakening trend. The weakening of the AMOC in recent years is consistent with Smeed et al. [2018], who used observational data of the AMOC from the RAPID line at 26°N and other observations in their study. The AMOC PC1 shows that the 2019 AMOC is the weakest in the 1990-2019 period.

Summary

The DFO-led annual oceanographic survey of the Labrador Sea provides observations of variability in the ocean climate and ventilation. The changes observed in the region are closely linked to the dynamics of the planetary climate system as a whole and affect the regional climate and ecosystems off Atlantic Canada. In June of 2019, the AR7W line was occupied by the Bedford Institute of Oceanography for the 32nd time since 1990. Additionally, the network of profiling Argo floats provided temperature and salinity data to 2000 m used for monitoring of year-round variability of the oceanographic conditions in the Labrador Sea. An omission of a single year (as happened in 2017) in precise systematic observations of the ocean state imposes significant limitation on the assessment, diagnosis and prediction of coast-to-coast full-depth environmental conditions in one of the most critical locations of the world ocean.

Key characteristics of the past and recent environmental conditions in the Labrador Sea are summarized in the scorecard shown in Figure 19, and are listed below:

1. The winter (Dec-Mar) NAO index in 2019 was above-normal. However, a low atmospheric pressure anomaly in the Labrador Sea in winter resulted in above-normal air temperatures. For SST, anomalies were near-normal in winter and above-normal in spring.
2. Sea ice extent anomalies in winter and spring were generally negative, except for a near-normal winter anomaly on the central Labrador Shelf.
3. In the Labrador Sea, surface heat losses in winter result in the formation of dense waters, which consequently spread across the ocean ventilating its deep layers and essentially driving the global ocean overturning circulation. In the winter of 2015, the Labrador Sea incurred the highest heat loss in more than two decades. However, the four following winters showed a significant reduction in the respective net surface heat losses, which remained above-normal in 2016 and 2017, but then declined to near-normal in 2018 and 2019.
4. Ocean temperature in the central Labrador Sea was above-normal, reversing a negative trend observed since 2010 in the 15-100 m layer, and since 2011 in the 200-2000 m layer. The earlier cooling of the deeper layer was primarily caused by deepening of winter convection, while the recent warming and convection weakening concur with the reduced 2019 winter heat loss.
5. Despite the persistent decline in the surface cooling since 2015, the water column preconditioned by a series of deep convection events eased the formation of a new Labrador Sea Water (LSW) that is seen as the most significant, in terms of volume and depth, since the mid-1990s.
6. The temperature and salinity profiles collected by research vessels and profiling Argo floats in the central Labrador Sea indicate that the developed 2019 winter mixed layer was shallower than in the period from 2014 to 2018, during which winter convection incrementally deepened from 1600 to 2000 m, respectively, turning out to be the deepest one since 1994 when the 80-year record convection depth of 2500 m was reached. As a result, the LSW year class developed during the pentad preceding 2019 is among the largest observed outside of the first pentad of the 1990s. In 2019, on the contrary, convection reached the depth of about 1400 m in the western part of the Labrador Basin, and only about 1000 m in the central and eastern parts. This also suggests that the near-normal winter convection in the winter of

2019 further added to gas (dissolved oxygen, anthropogenic gases, and carbon dioxide) uptake and consequently respective gas concentrations in the Labrador Sea in the upper 1000 m layer.

7. Model results suggest that the transport of the Labrador Current decreased between 1995 and 2014, but has since increased slightly. A weakening trend of the AMOC since mid-1990s is obtained in this model hindcast. Continuing weakening of the AMOC in recent years is present, which leads to the weakest AMOC in 2019 from this model simulation.

Acknowledgements

We thank the officers and the crews of the Canadian Coast Guard vessels for their dedicated help in keeping the Labrador Sea survey running. We are grateful to the reviewers for their helpful comments and suggestions. The NCEP Reanalysis data were provided by the NOAA-CIRES Climate Diagnostics Center, Boulder, Colorado, USA, and the sea ice concentration data were provided by the US National Snow and Ice Data Center.

Tables

Table 1. Oceanographic Labrador Sea cruises conducted by the Bedford Institute of Oceanography since 1990 as part of WOCE, CLIVAR, AZOMP

Cruise Name	Vessel	Project	Chief Scientist	Cruise Dates
HUD-92-014	CCGS Hudson	WOCE	John Lazier	27-May – 15-Jun, 1992
HUD-95-011	CCGS Hudson	WOCE	John Lazier	7-Jun – 5-Jul, 1995
HUD-96-006	CCGS Hudson	WOCE	John Lazier	10-May – 2-Jun, 1996
HUD-96-026	CCGS Hudson	WOCE	Allyn Clarke	15-Oct – 20-Nov, 1996
HUD-97-009	CCGS Hudson	WOCE/JGOFS	Allyn Clarke	9-May – 12-Jun, 1997
HUD-98-023	CCGS Hudson	WOCE/CLIVAR	John Lazier	22-Jun – 10-Jul, 1998
HUD-99-022	CCGS Hudson	Climate	Allyn Clarke	27-Jun – 14-Jul, 1999
HUD2000009	CCGS Hudson	Climate	Allyn Clarke	20-May – 8-Jun, 2000
HUD2001022	CCGS Hudson	Climate	Allyn Clarke	30-May – 15-Jun, 2001
HUD2002032	CCGS Hudson	Climate	Allyn Clarke	23-Jun – 19-Jul, 2002
HUD2002075	CCGS Hudson	Biology/Climate	Erica Head	29-Nov – 12-Dec, 2002
HUD2003038	CCGS Hudson	Climate	Allyn Clarke	13-Jul – 4-Aug, 2003
HUD2004016	CCGS Hudson	Climate	Allyn Clarke	14-May – 30-May, 2004
HUD2005016	CCGS Hudson	Climate	Allyn Clarke	27-May – 7-Jun, 2005
HUD2006019	CCGS Hudson	Climate	Ross Hendry	24-May – 8-Jun, 2006
HUD2007011	CCGS Hudson	Climate	Ross Hendry	10-May – 29-May, 2007
HUD2008009	CCGS Hudson	Climate	Glen Harrison	20-May – 4-Jun, 2008
HUD2009015	CCGS Hudson	AZOMP	Glen Harrison	18-May – 1-Jun, 2009
HUD2010014	CCGS Hudson	AZOMP	Glen Harrison	13-May – 30-May, 2010
HUD2011009	CCGS Hudson	AZOMP	Igor Yashayaev	6-May – 29-May, 2011
MLB2012001	CCGS M.L. Black	AZOMP	Igor Yashayaev	25-Jun – 20-Jul, 2012
HUD2013008	CCGS Hudson	AZOMP	Igor Yashayaev	4-May – 28-May, 2013
HUD2014007	CCGS Hudson	AZOMP	Igor Yashayaev	2-May – 26-May, 2014
HUD2015006	CCGS Hudson	AZOMP	Igor Yashayaev	1-May – 26-May, 2015
HUD2016006	CCGS Hudson	AZOMP	Igor Yashayaev	30-Apr – 24-May, 2016
HUD2018008	CCGS Hudson	AZOMP	Igor Yashayaev	25-Apr – 20-May, 2018
AMU2019001	CCGS Amundsen	AZOMP	Igor Yashayaev	2-Jun – 19-June, 2019

Figures

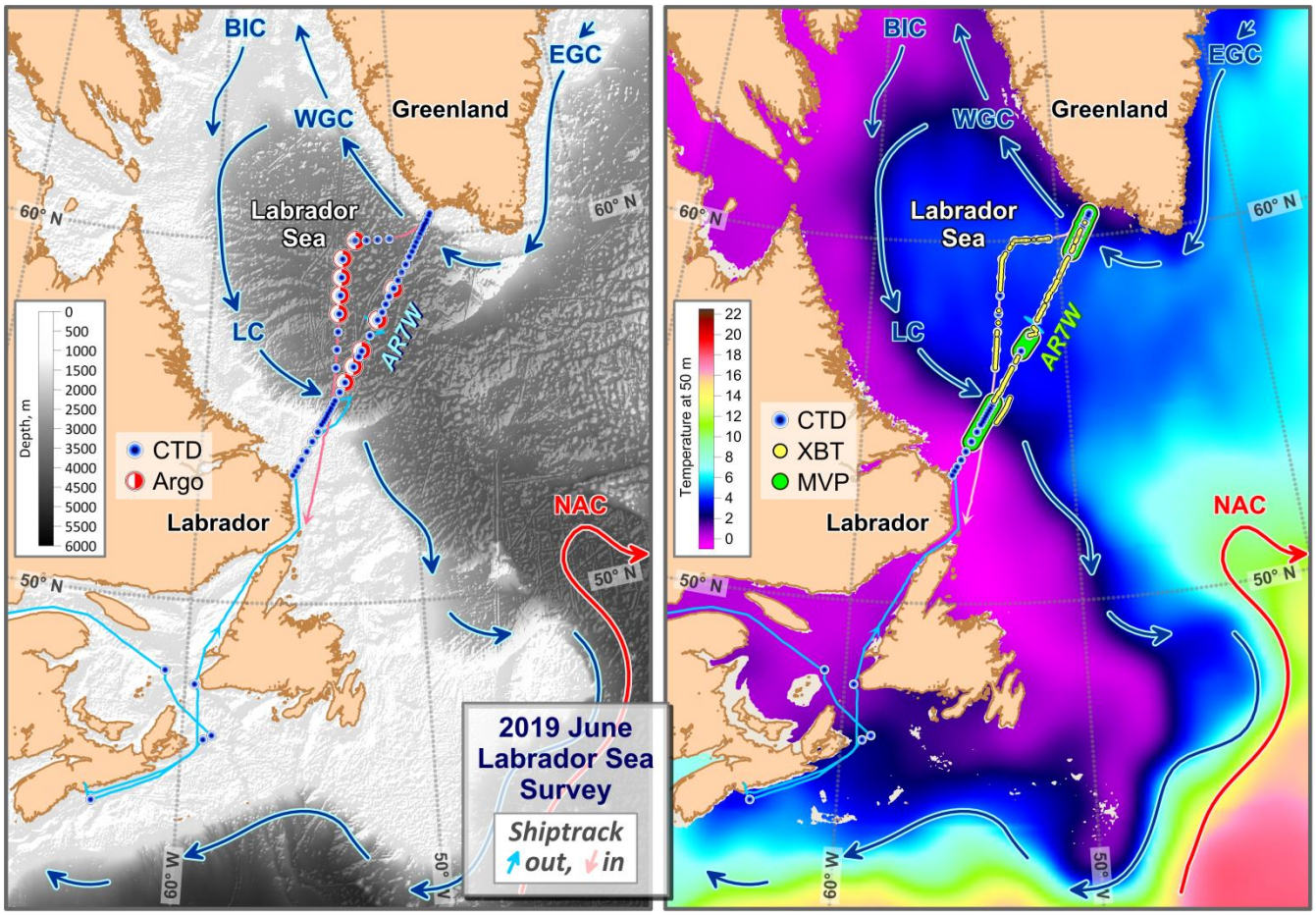

Figure 1. Topography (left panel), long-term mean temperature at 50 m (right panel) and surface currents in the Labrador Sea and adjacent regions of the North Atlantic. The 2019 June Labrador Sea mission CTD stations (both panels), Argo float deployment sites (left panel), XBT profiles (right panel) and MVP transects (right panel).

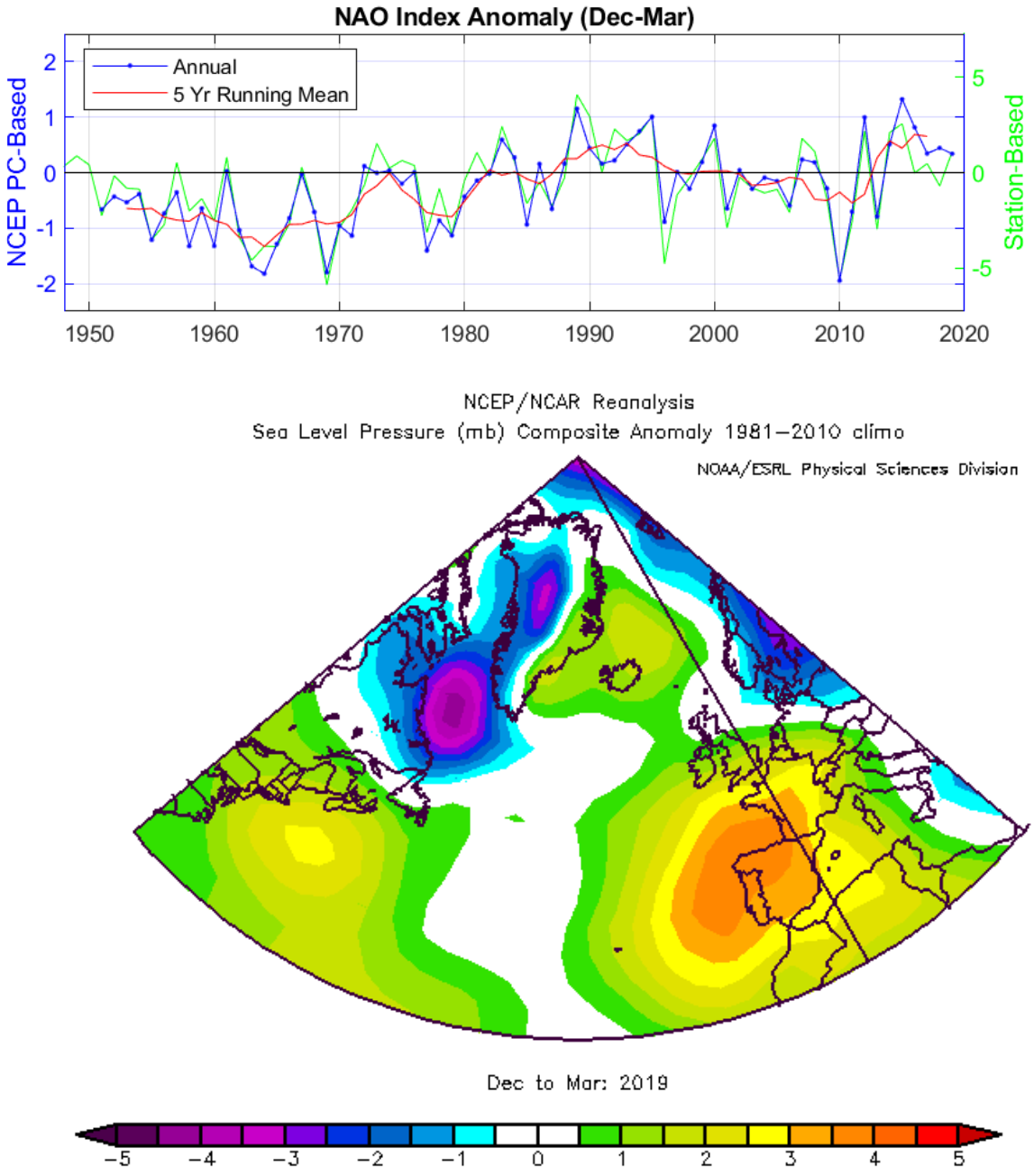

Figure 2. Anomalies of the North Atlantic Oscillation (NAO) index, relative to the 1981-2010 mean. The station-based NAO index (green) is defined as the winter (December, January, February, March) sea level pressure difference between the Azores and Iceland; data were obtained from https://climatedataguide.ucar.edu/climate-data/hurrell-north-atlantic-oscillation -nao-index-station-based (Hurrell et al. 2018). The PC-based NAO index (blue) is associated with the first empirical orthogonal function (EOF) of standardized monthly 500-mb height anomaly fields for the Northern Hemisphere; data were obtained from https://www.cpc.ncep.noaa.gov/data/teledoc/nao.shtml. The lower panel shows the 2019 December-March sea level pressure anomaly over the North Atlantic.

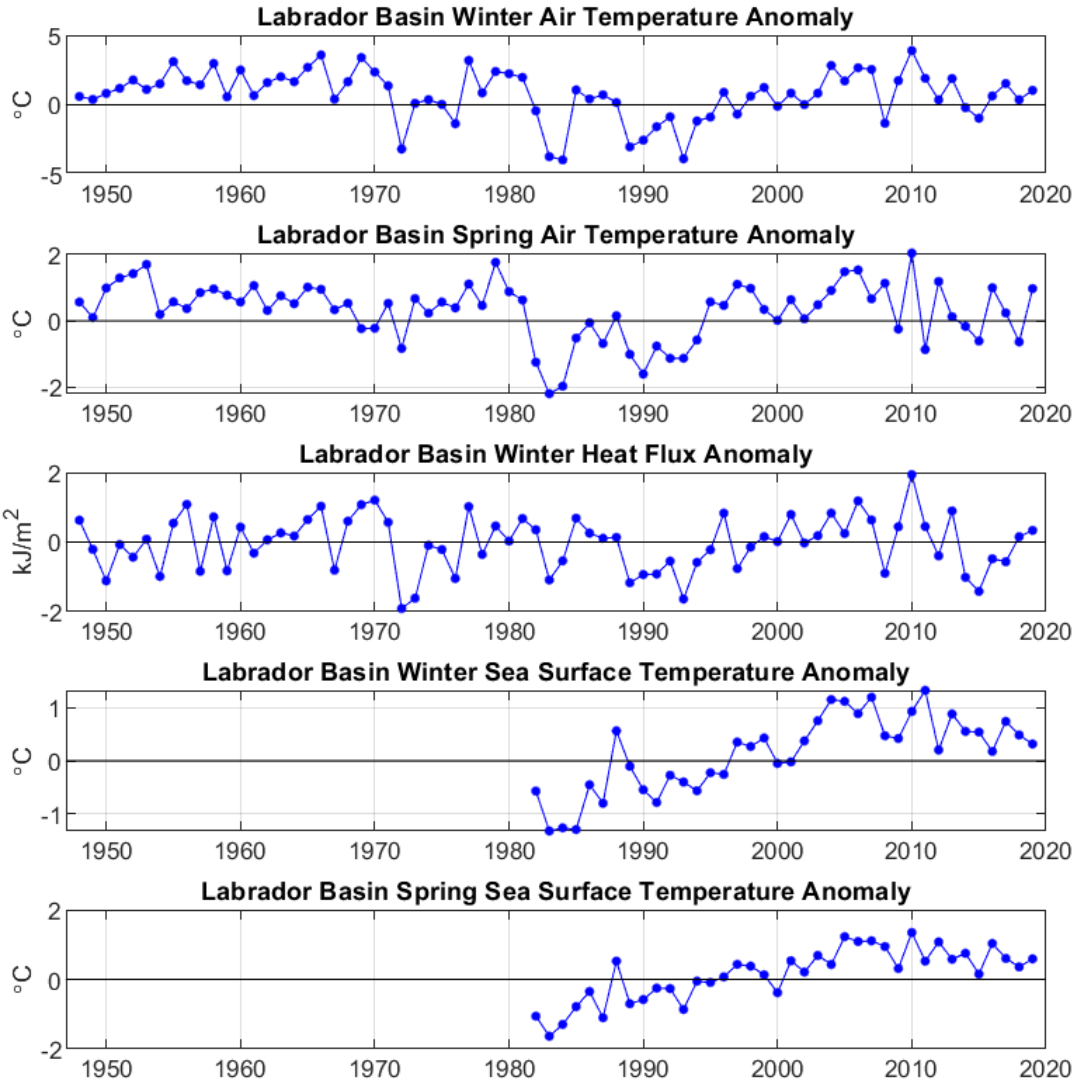

Figure 3. Anomalies of Labrador Basin winter and spring air temperature, cumulative winter surface heat flux, and winter and spring sea surface temperature, relative to the 1981-2010 mean.

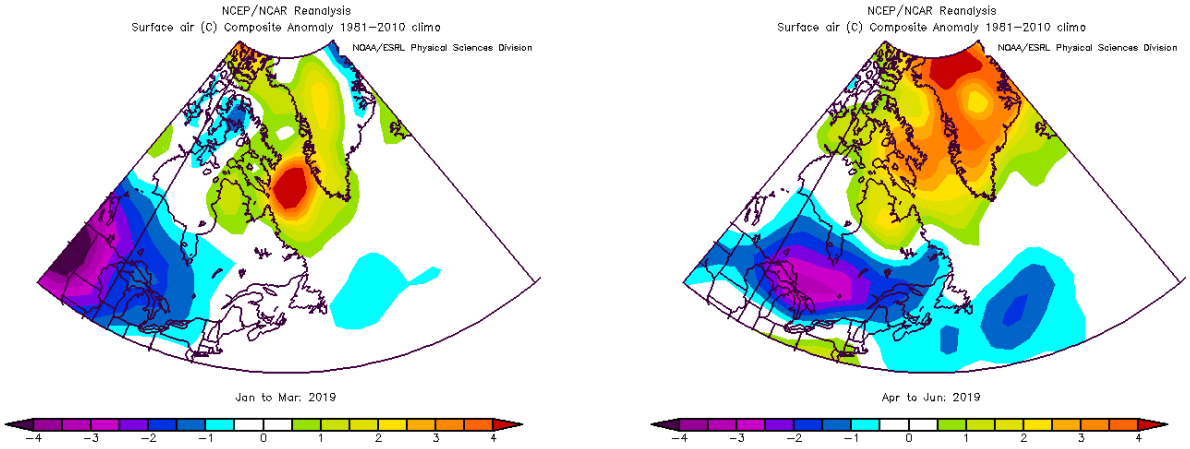

Figure 4. Winter and spring air temperature anomalies (ºC) over the Northwest Atlantic relative to the 1981-2010 means; data were obtained from NOAA Internet site (accessed 30 April 2019).

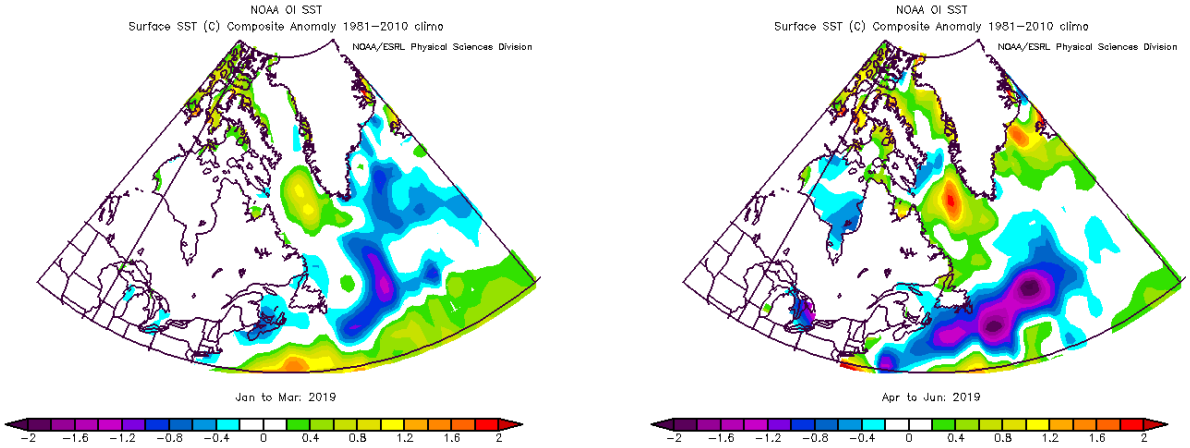

Figure 5. Winter and spring sea surface temperature anomalies (ºC) over the Northwest Atlantic relative to the 1981-2010 means; data were obtained from NOAA Internet site (accessed 04 Feb 2020).

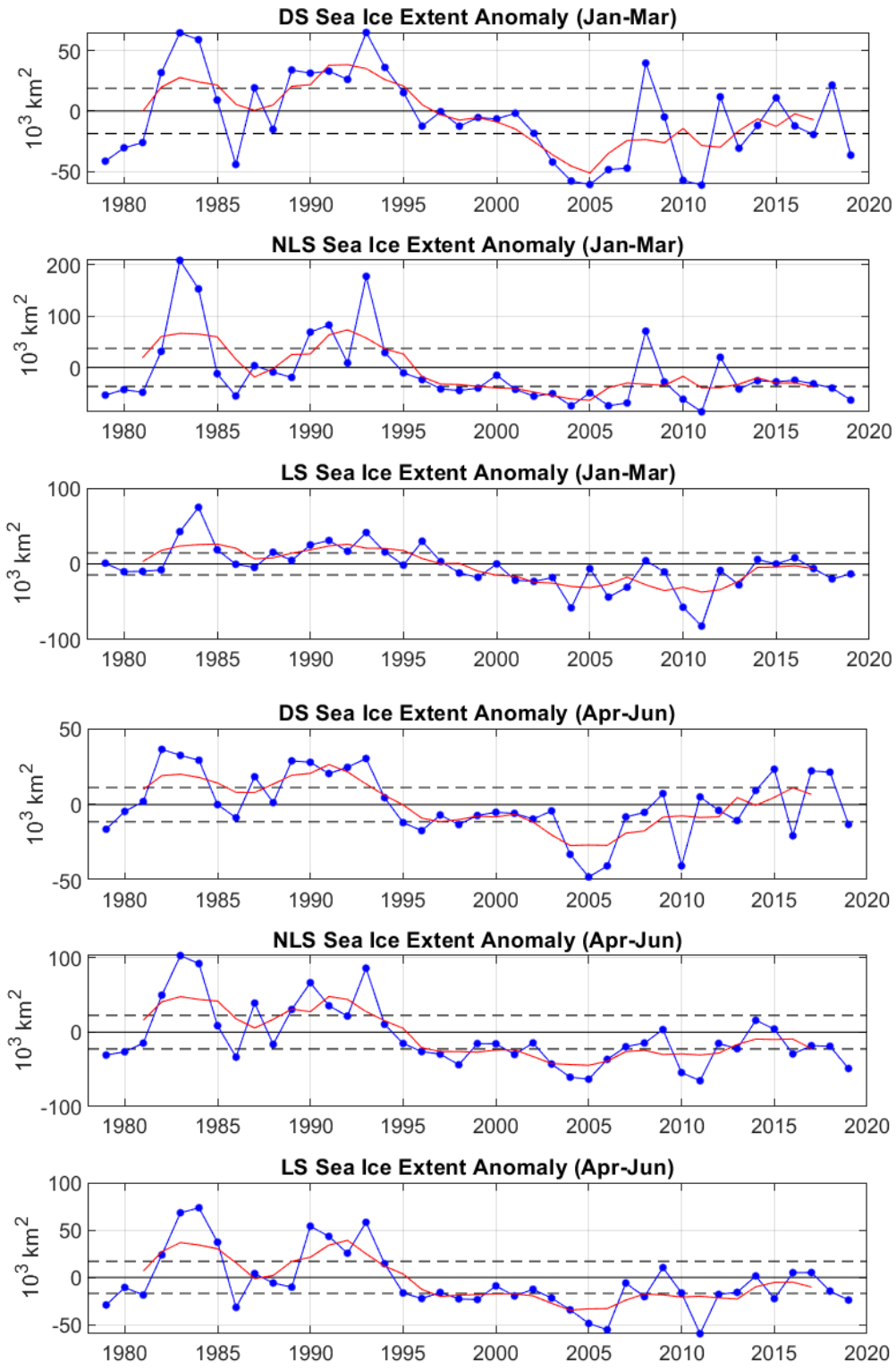

Figure 6. Winter and spring sea ice extent anomalies (blue) and their five year running means (red) for: (1) Davis Strait (63-68°N), (2) the Northern Labrador Sea (58-63°N), and (3) Labrador Shelf (53-58°N). Horizontal dashed lines represent plus or minus 0.5 SD for the 1981-2010 period.

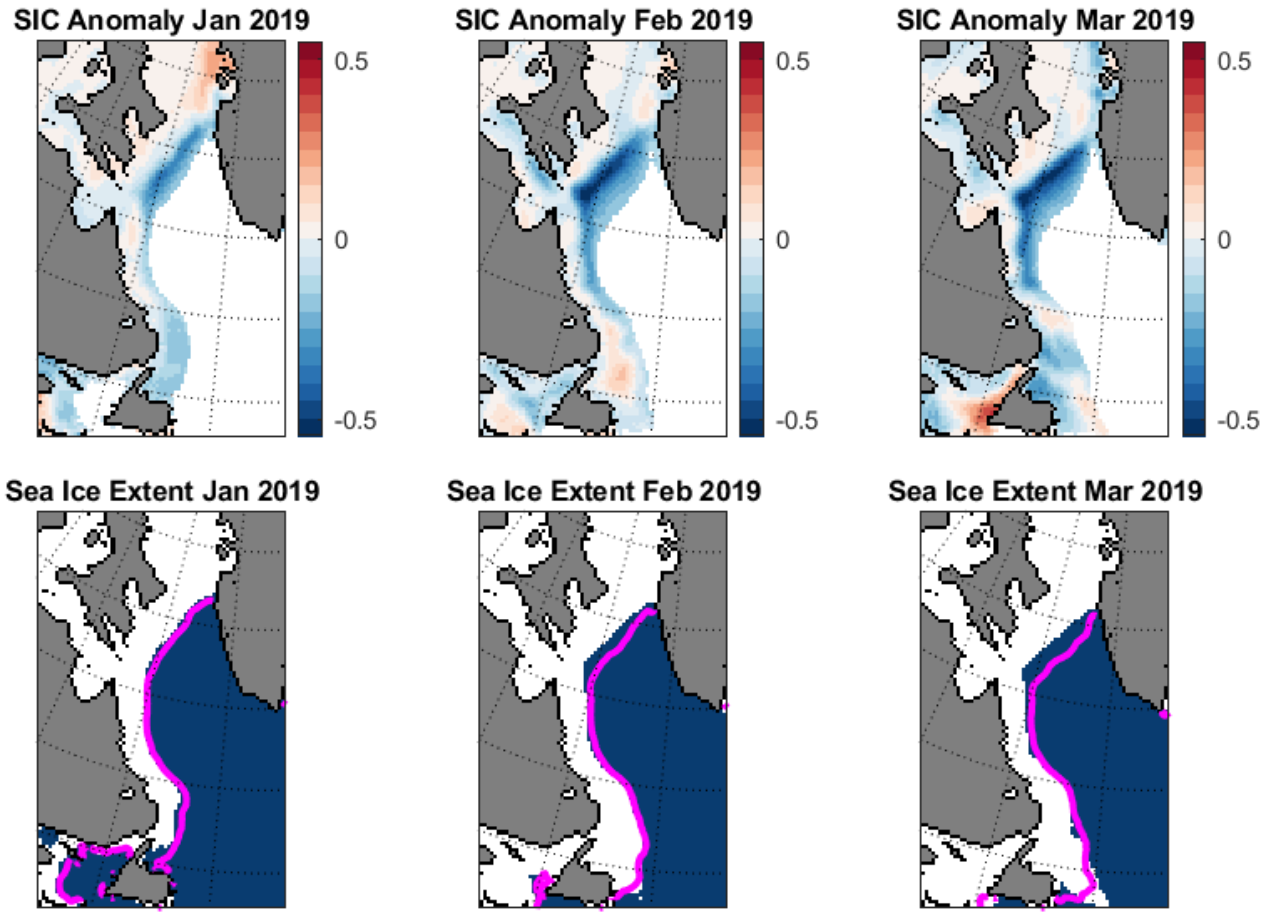

Figure 7. Sea ice concentration anomalies (top) and sea ice extent (bottom) for January-March 2019 as derived by the US National Snow and Ice Data Center (reference period 1979-2000) http://nsidc.org/. The magenta lines show the median ice edge for 1981-2010.

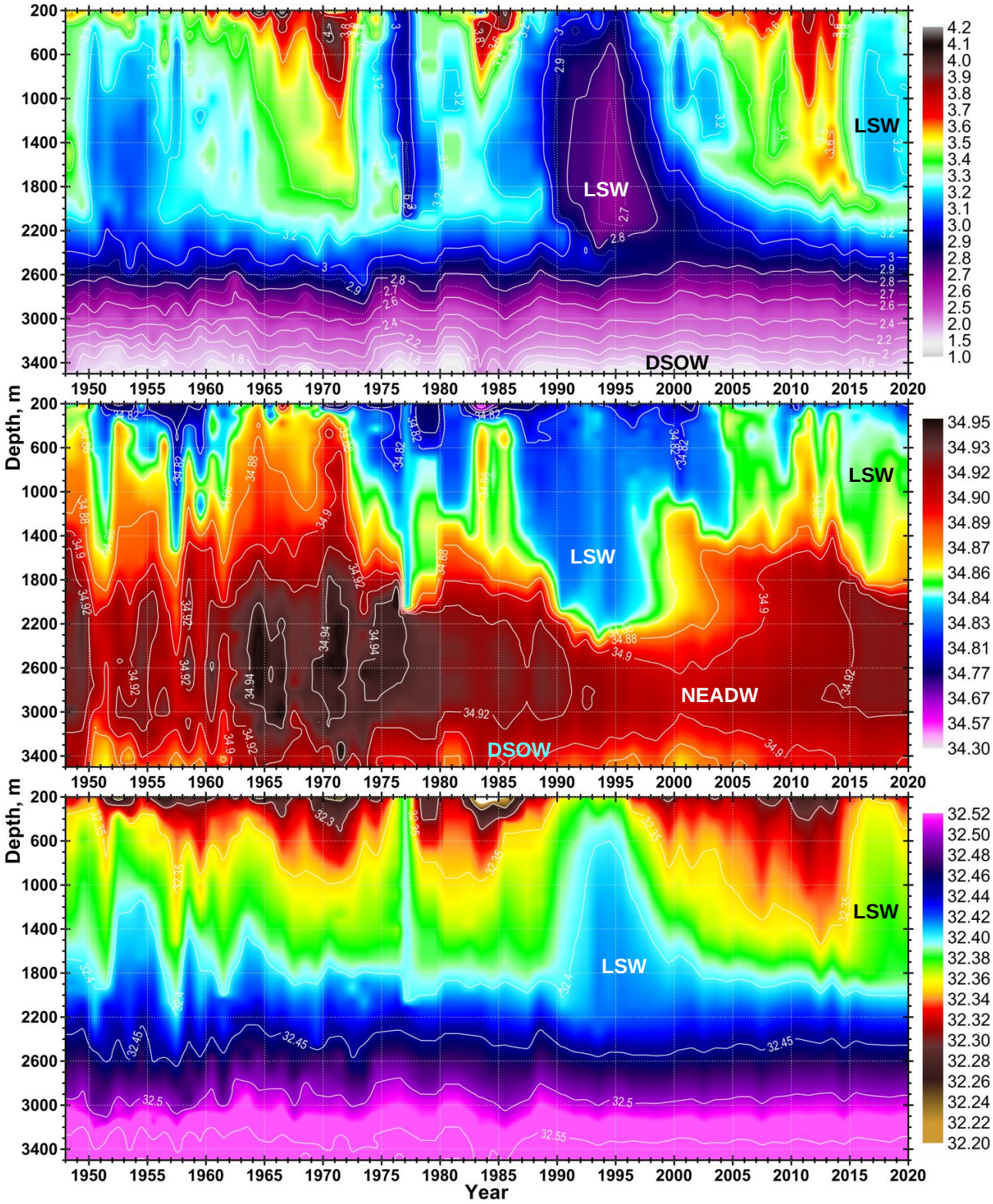

Figure 8. Annual temperature (upper panel), salinity (middle panel) and density (w.r.t. 1000 dbar, lower panel) means in the central region of the Labrador Sea between 200 and 3500 m based on profiling Argo float and shipboard observations for the time period of 1948-2019. LSW, NEADW and DSOW indicate Labrador Sea Water, Northeast Atlantic Deep Water and Denmark Strait Overflow Water, respectively.

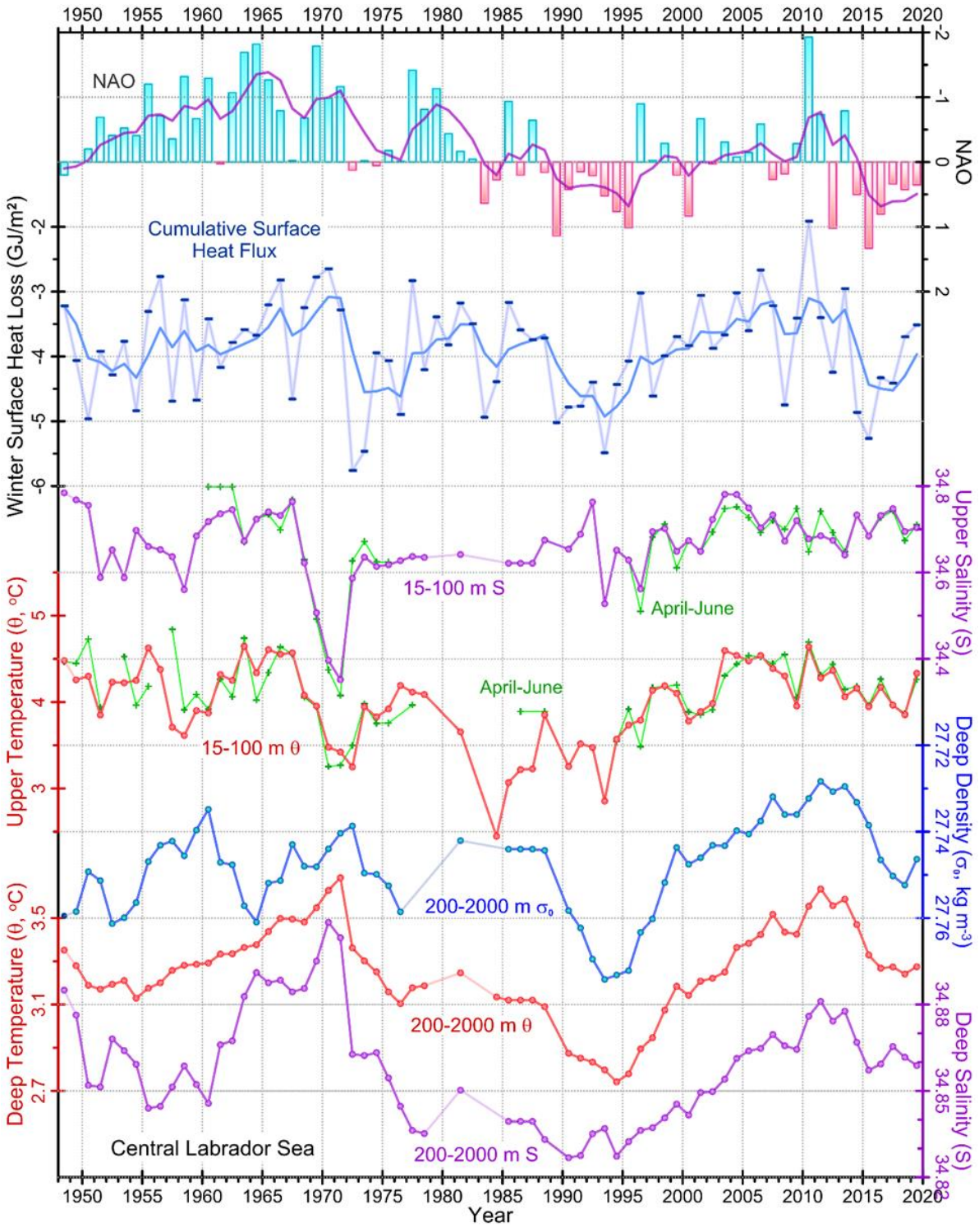

Figure 9. Major environmental indices for the central Labrador Sea since 1948. From top down: The normalized winter NAO index (upper bar graph, inverted scale); The NCEP-based cumulative surface heat flux computed for the central Labrador Sea over individually-defined annual cooling seasons (blue); The upper two solid lines indicate five-back-point filtered series; Annual and spring mean temperature (θ) and salinity (S) averaged over the 15-100 m depth range, and annual mean θ, S and density (σ_0, w.r.t. 0 dbar) averaged over the 200–2000 m depth range in the central Labrador Sea.

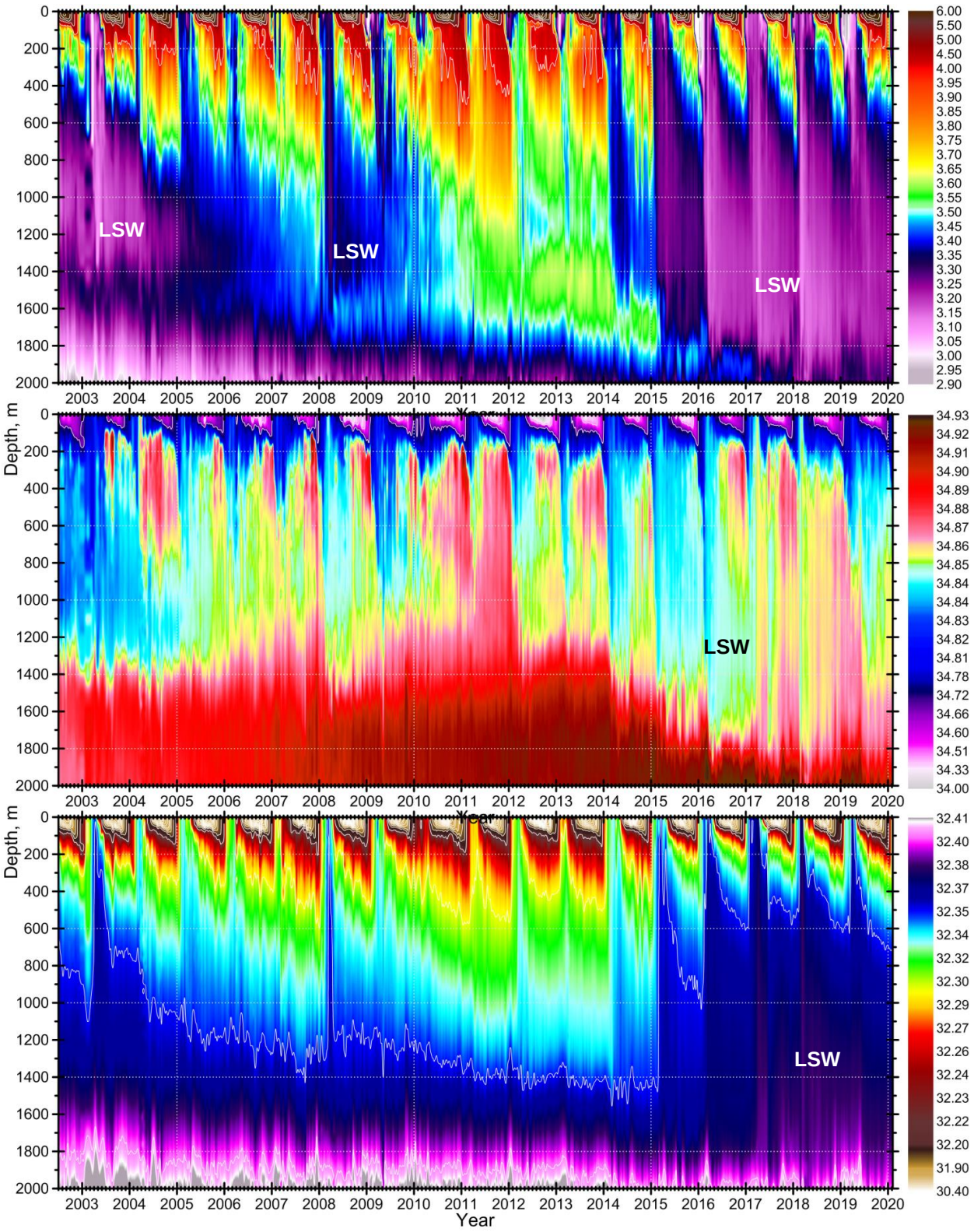

Figure 10. Variability of temperature (upper panel), salinity (lower panel) and density (middle panel) in the central region of the Labrador Sea based on profiling Argo float and research vessel survey data from 0 to 2000 m for the time period of 2002-2020. These plots were constructed without temporal averaging.

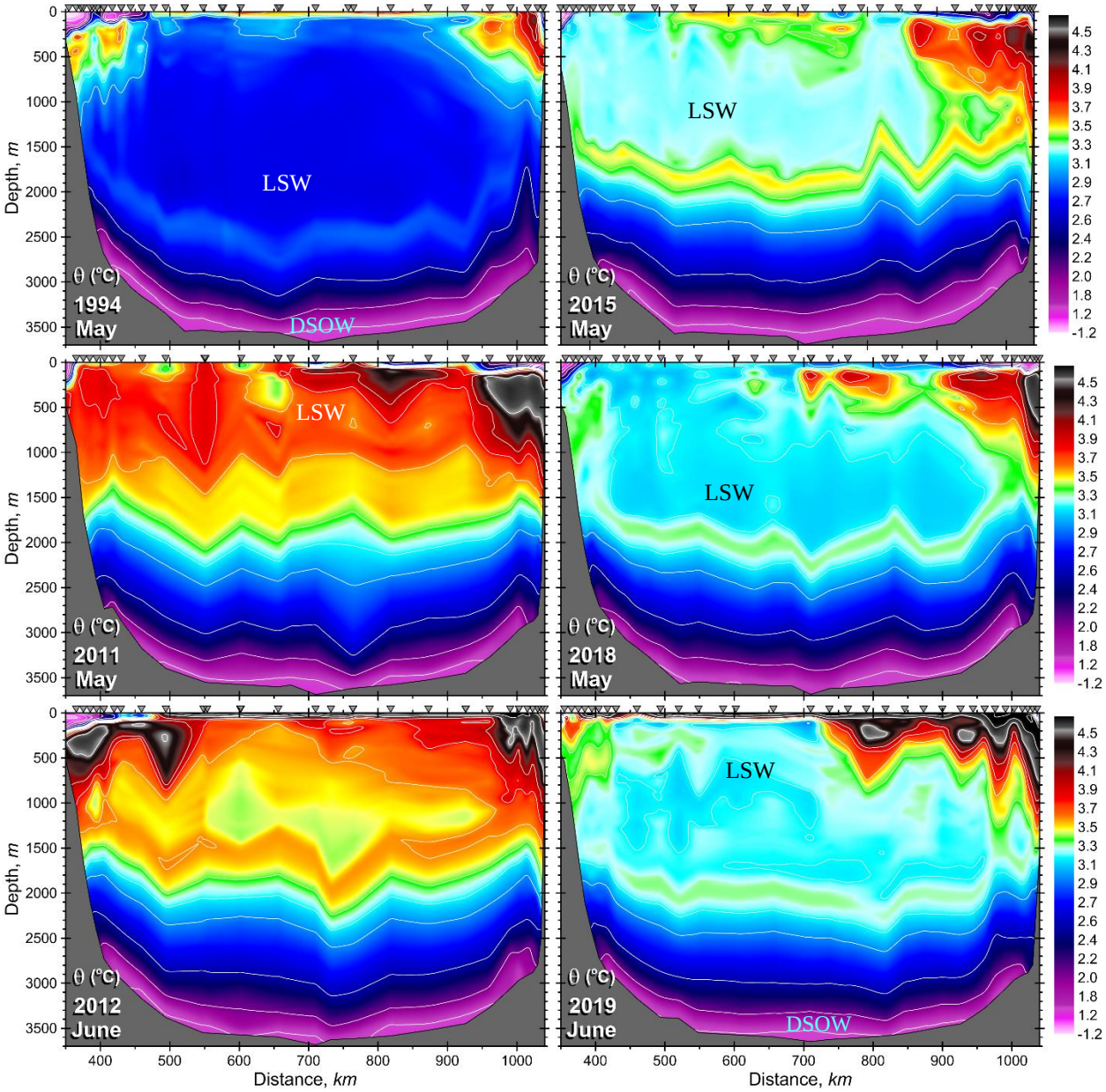

Figure 11. Distributions of potential temperature (θ, °C) on the AR7W line across the Labrador Sea from annual spring-summer surveys in 1994, 2011, 2012, 2015, 2018 and 2019. Inverted triangles along the top of each panel indicate station locations. LSW, NEADW and DSOW indicate Labrador Sea Water, Northeast Atlantic Deep Water and Denmark Strait Overflow Water, respectively.

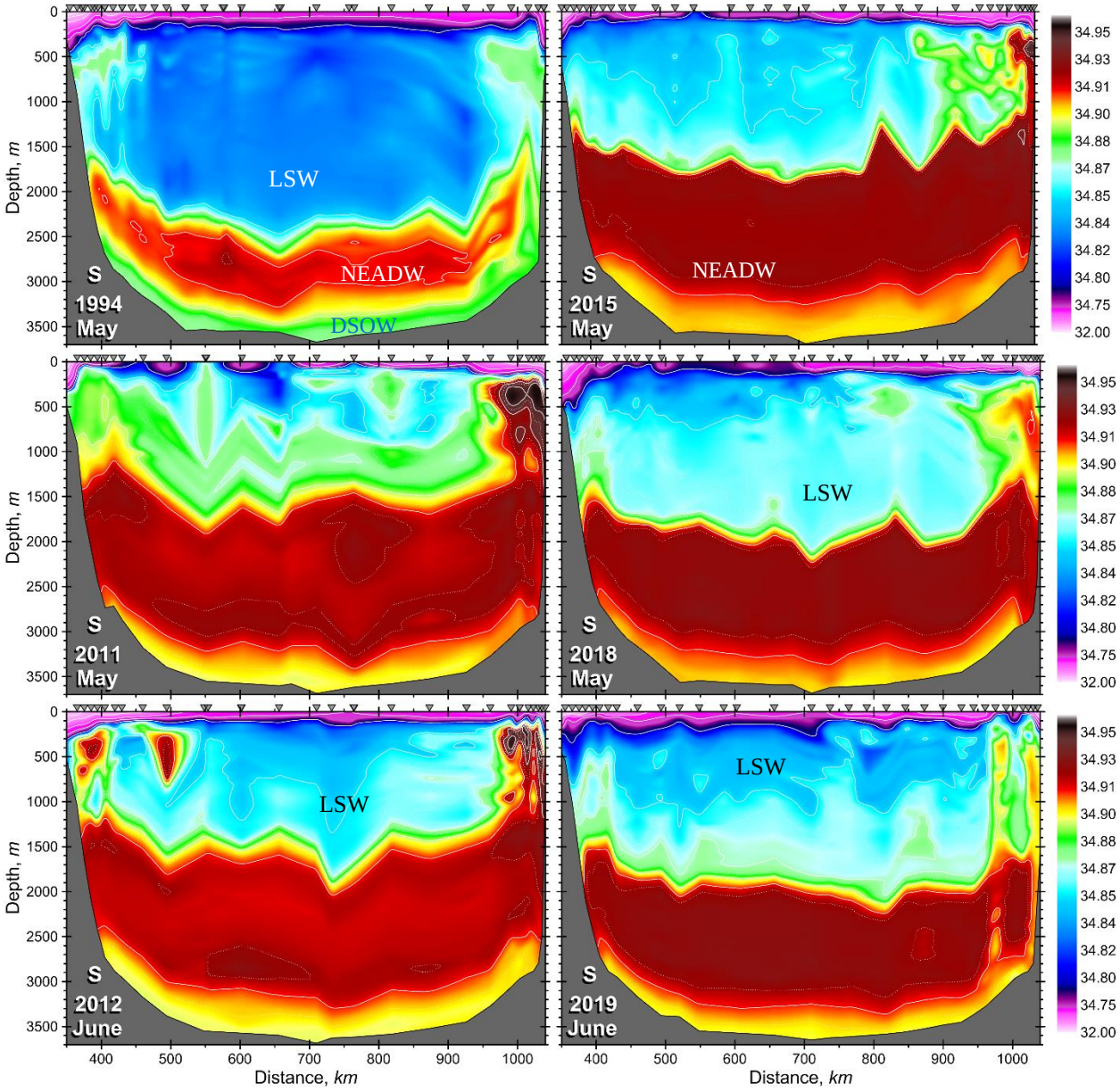

Figure 12. Distributions of salinity (S) on the AR7W line across the Labrador Sea from annual spring-summer surveys in 1994, 2011, 2012, 2015, 2018 and 2019. Inverted triangles along the top of each panel indicate station locations. LSW, NEADW and DSOW indicate Labrador Sea Water, Northeast Atlantic Deep Water and Denmark Strait Overflow Water, respectively.

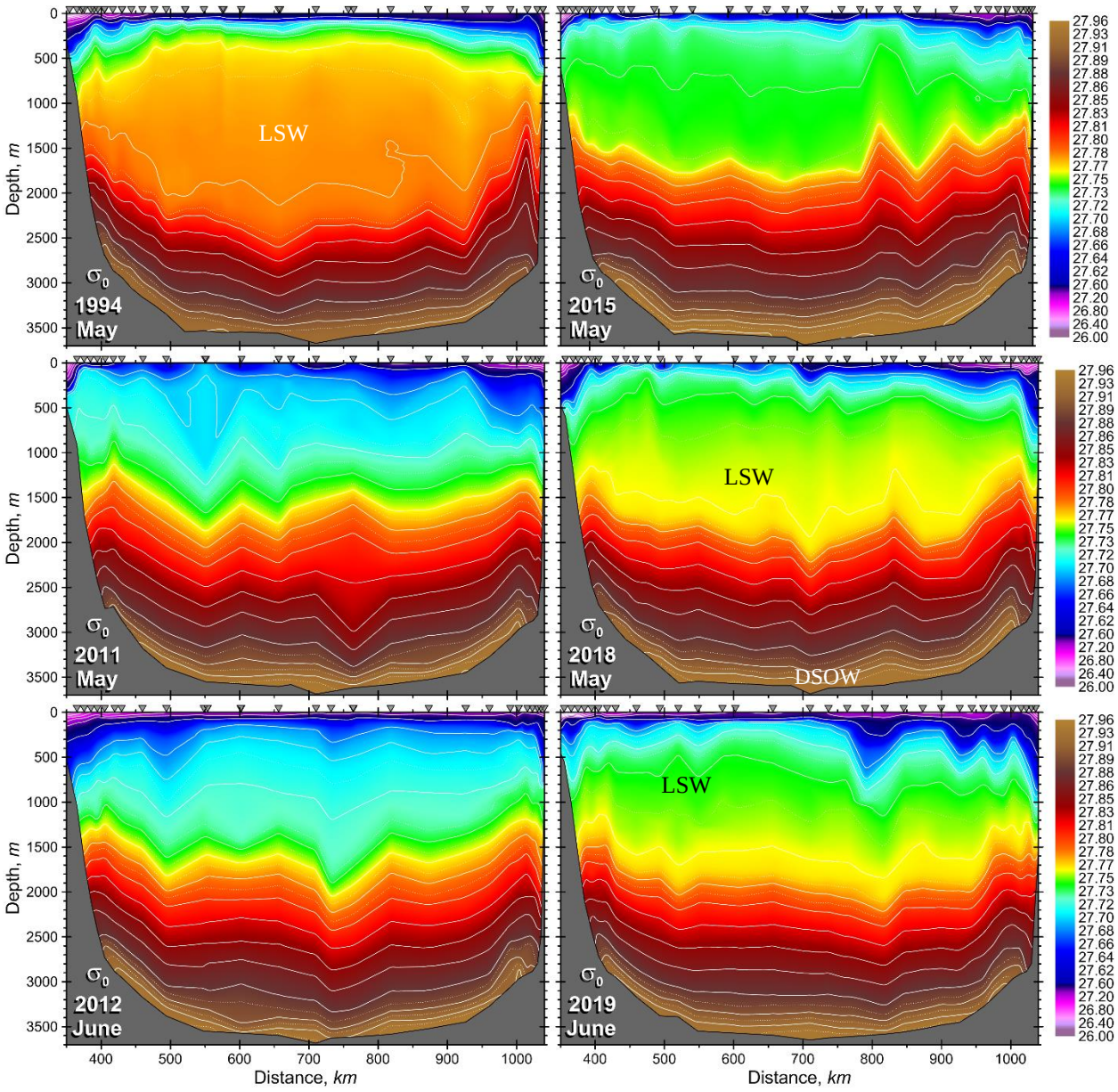

Figure 13. Distributions of potential density (σ_o, referenced to the sea surface, kg/m3) on the AR7W line across the Labrador Sea from annual spring-summer surveys in 1994, 2011, 2012, 2015, 2018 and 2019. Inverted triangles along the top of each panel indicate station locations. LSW, NEADW and DSOW indicate Labrador Sea Water, Northeast Atlantic Deep Water and Denmark Strait Overflow Water, respectively.

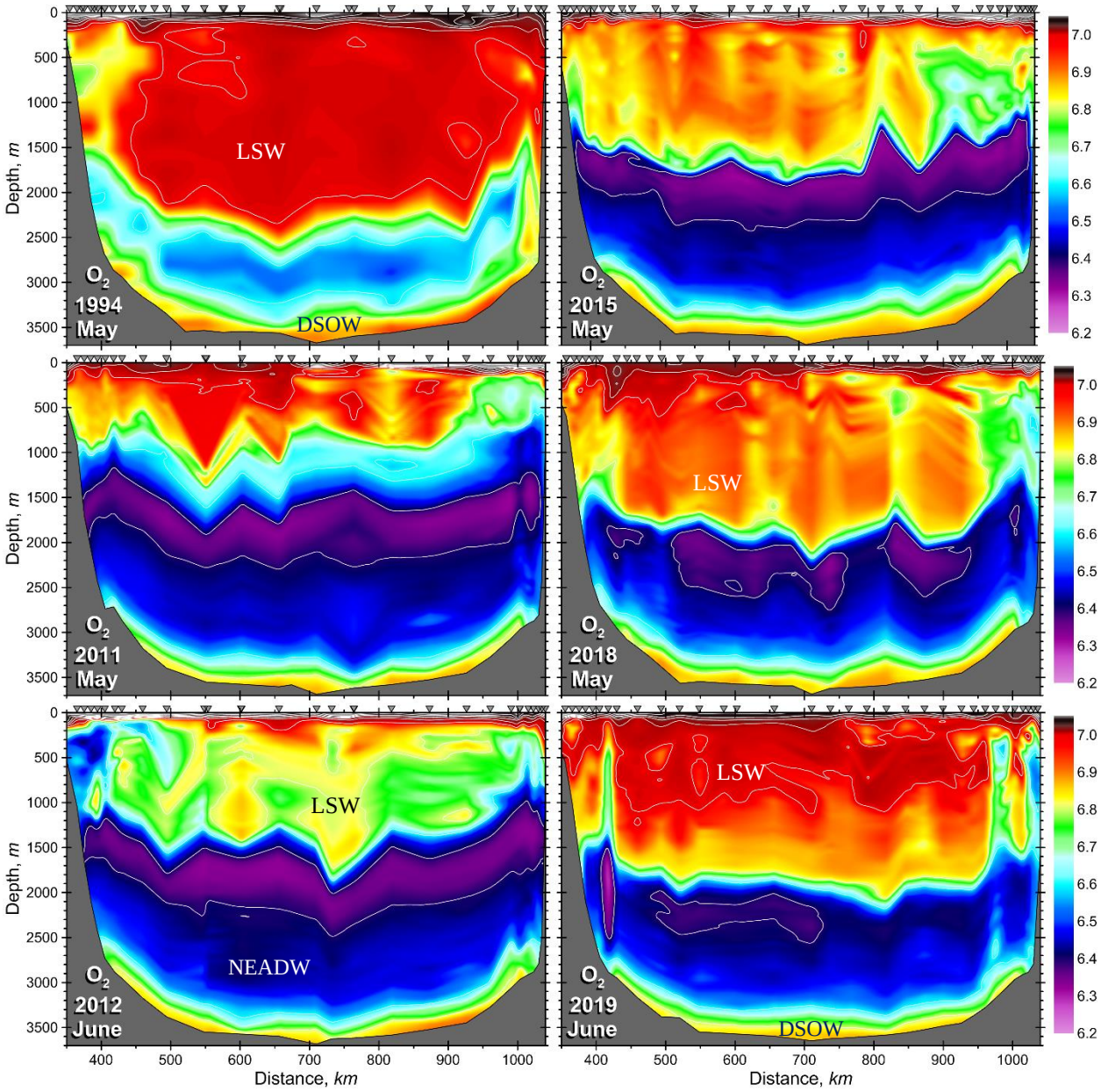

Figure 14. Distributions of dissolved oxygen (ml/l) on the AR7W line across the Labrador Sea from annual spring-summer surveys in 1994, 2011, 2012, 2015, 2018 and 2019. Inverted triangles along the top of each panel indicate station locations. LSW, NEADW and DSOW indicate Labrador Sea Water, Northeast Atlantic Deep Water and Denmark Strait Overflow Water, respectively.

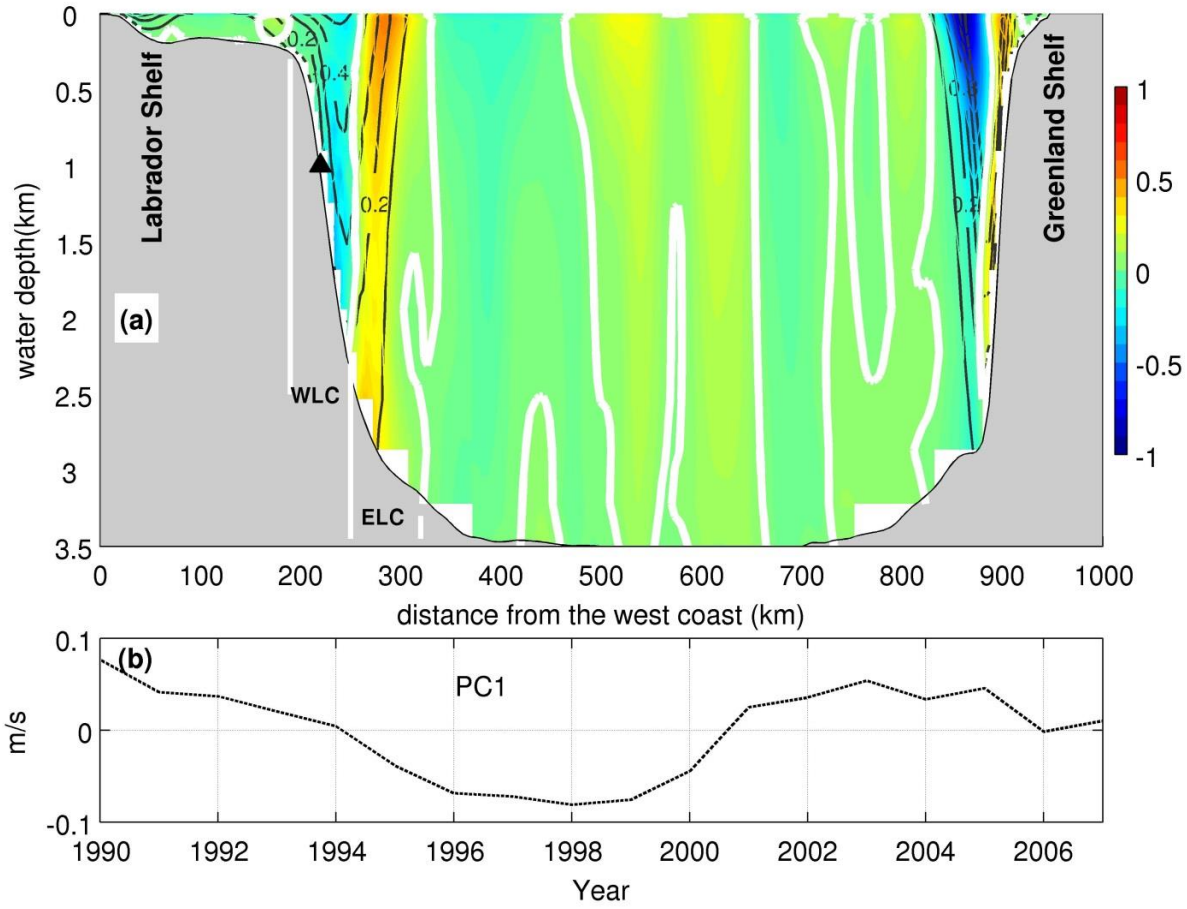

Figure 15. (a) EOF1 pattern of the normal velocities along AR7W (based on results from 1990 to 2007). The shaded areas represent the EOF pattern, bold white lines are zeros contours of the EOF pattern, the black labeled lines are the mean normal velocities (in m/s). Note: positive direction is northward. The black triangle indicates the location of the mooring referred to in the text. (b) Corresponding PC1.

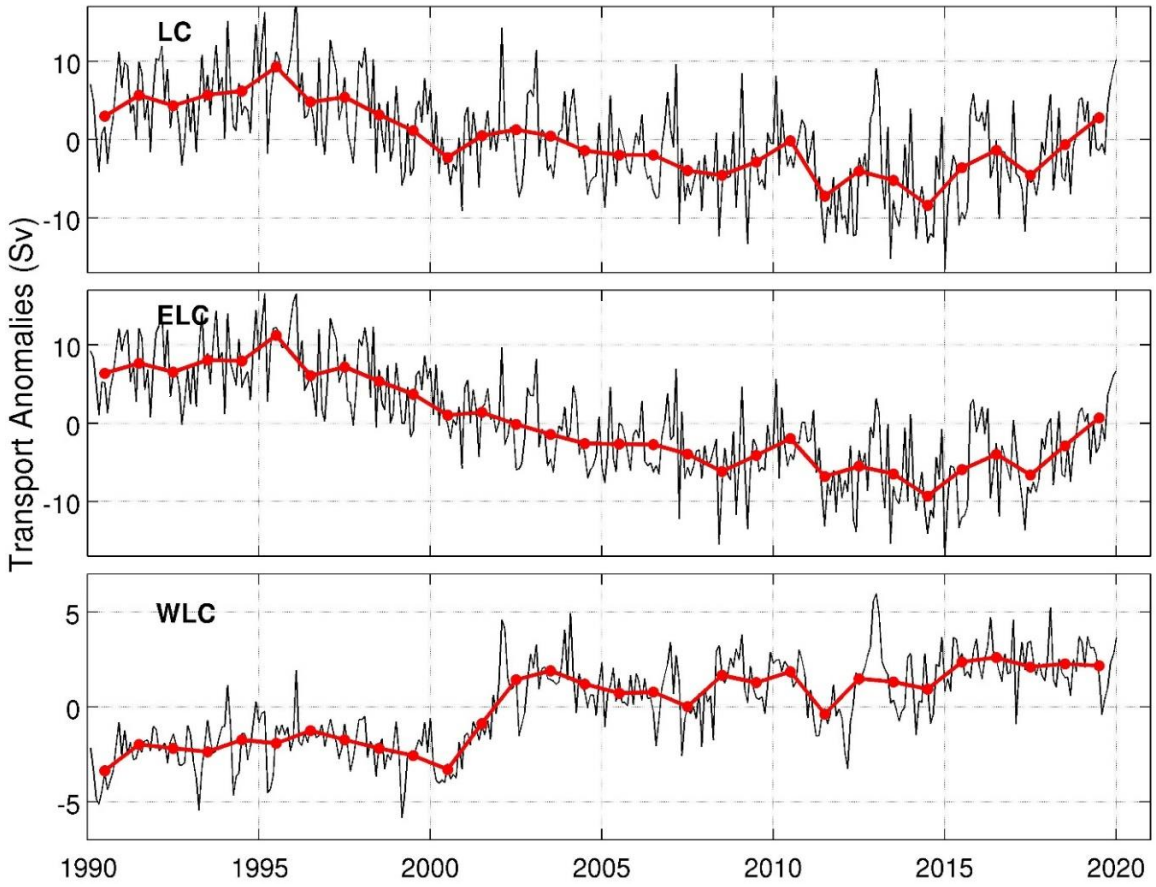

Figure 16. Transport anomalies of the LC, ELC, and WLC from 1990 to 2019.
Note: black lines are from the monthly data, and red lines and dots are from the annual means.

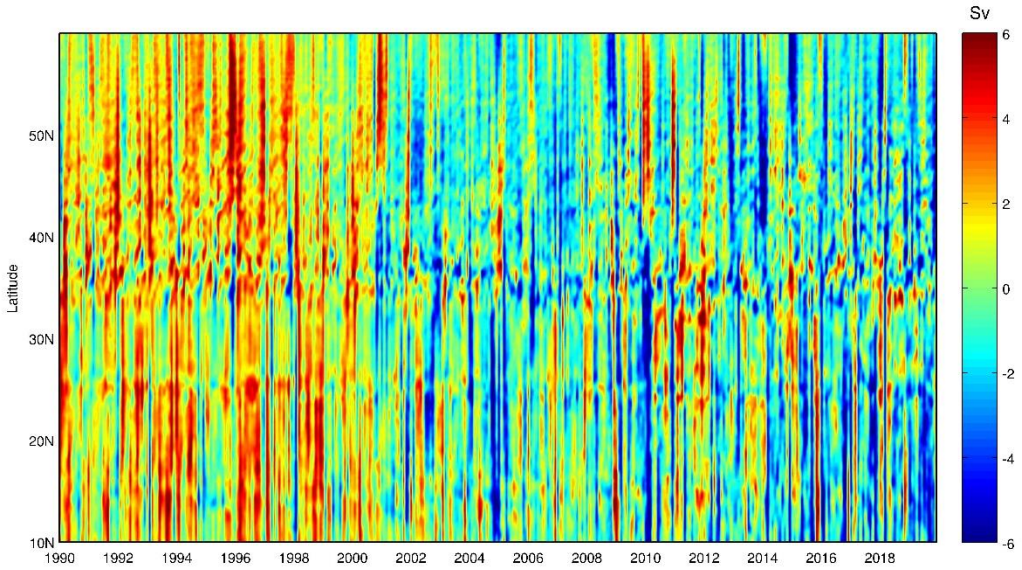

Figure 17. The AMOC anomalies at different latitudes with the seasonal cycles removed, but without detrending.

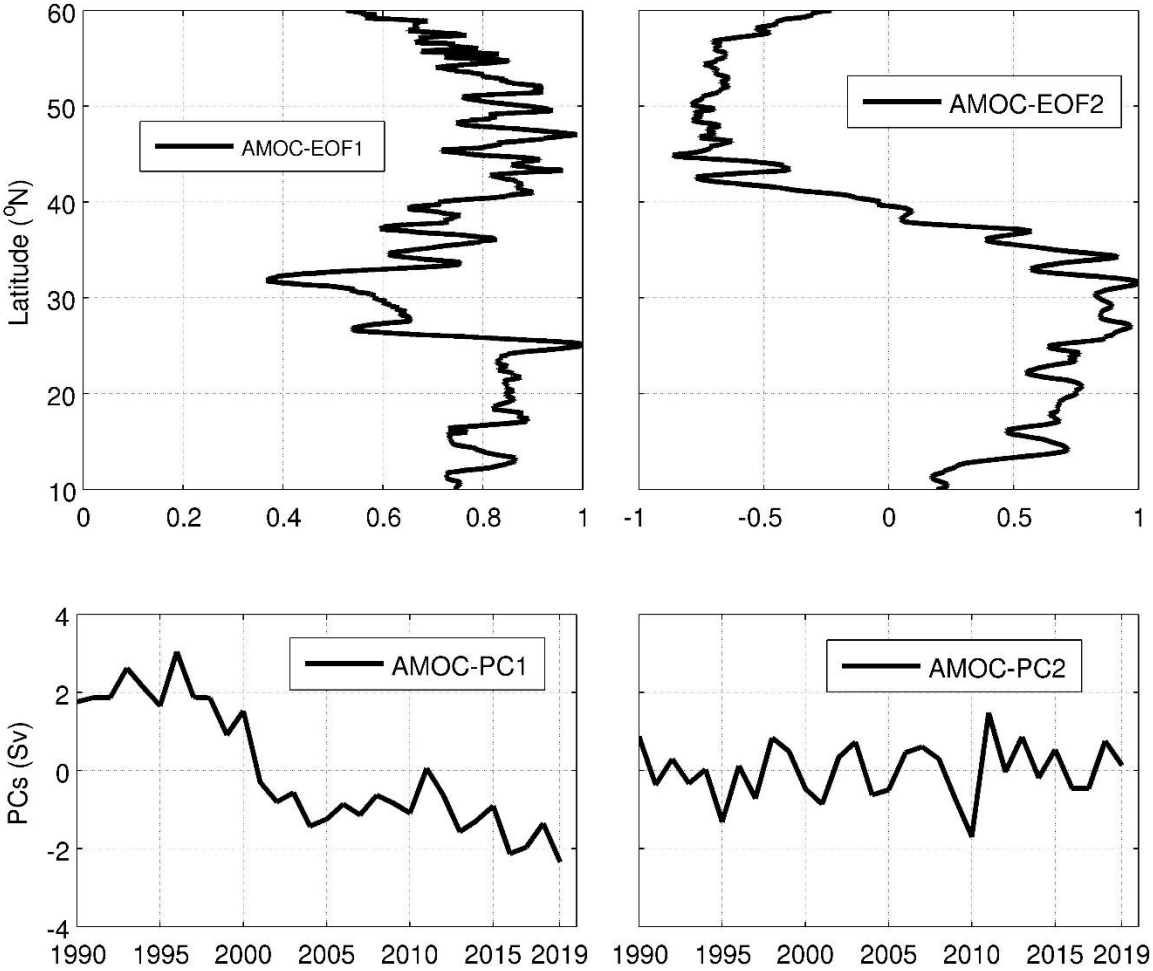

Figure 18. EOF patterns of AMOC (top panel) and associated PCs of these EOFs (bottom panel).

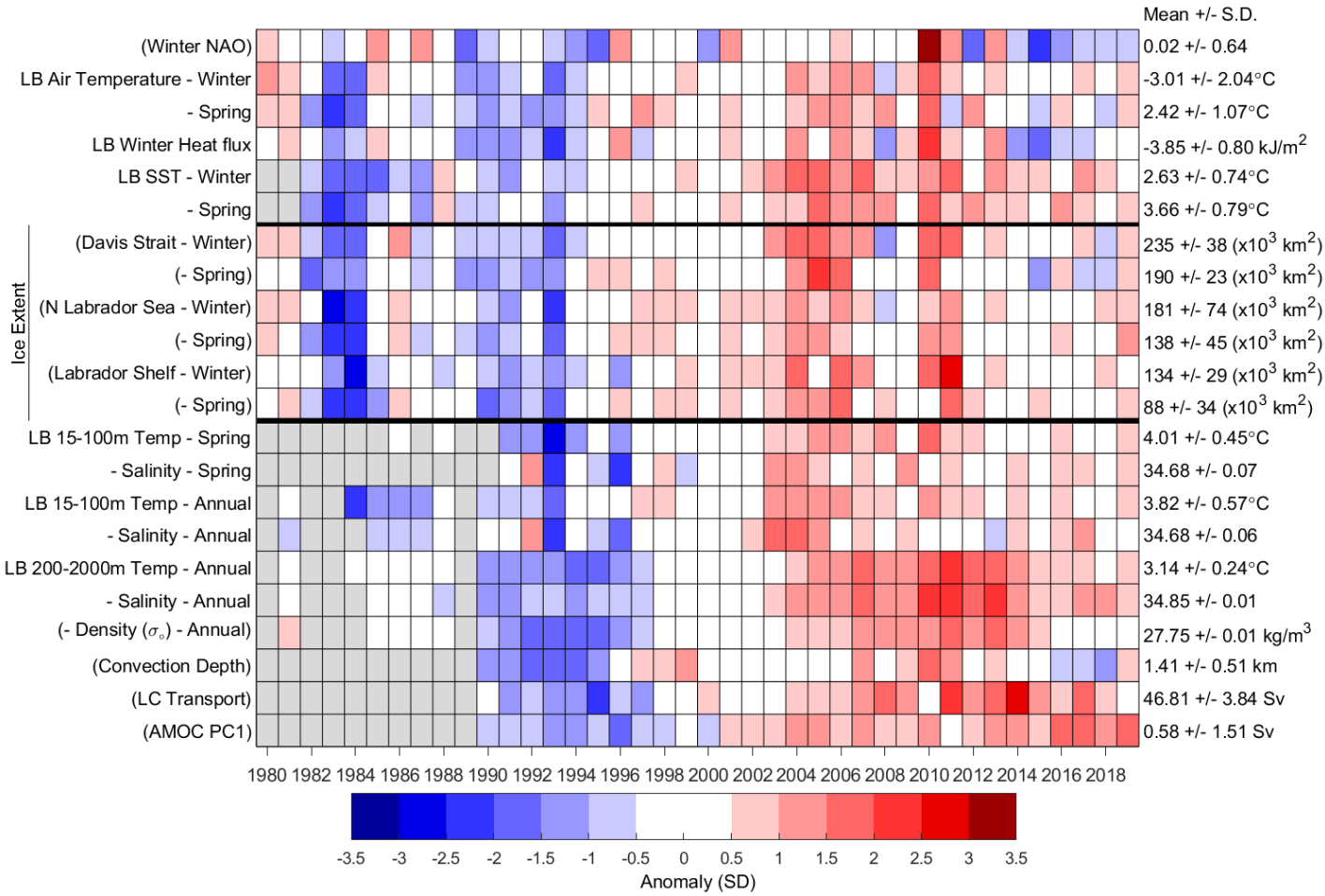

Figure 19. Scorecard for 1980-2019 oceanographic series. A grey cell indicates missing data, a white cell is a value within 0.5 SD of the long-term mean based on data from 1981–2010 when possible; a red cell indicates above normal conditions, and a blue cell below normal. Variables whose names appear in parentheses have reversed colour coding, whereby reds are lower than normal values that correspond to warm conditions. More intense colours indicate larger anomalies. Long-term means and standard deviations are shown on the right-hand side of the figure. North Atlantic Oscillation [NAO], Labrador Basin [LB], Labrador Current [LC].

References

Arctic-Subarctic Ocean Fluxes: Defining the Role of the Northern Seas in Climate, 2008, Edited by Robert R. Dickson, Jens Meincke, Peter Rhines, Springer Science & Business Media, March 4, 2008, 736 pages.

Bindoff, N. L., Willebrand, J., Artale, V., Cazenave, A., Gregory, J., Gulev, S., Hanawa, K., Le Quéré, C., Levitus, S., Nojiri, Y., Shum, C. K., Talley, L. D. and Unnikrishnan A. 2007. Chapter 5. Observations: Oceanic Climate Change and Sea Level, Climate Change 2007: The Physical Science Basis, Contribution of Working Group I to the Fourth Assessment Report of the Intergovernmental Panel on Climate Change, [Solomon, S., D. Qin, M. Manning, Z. Chen, M. Marquis, K.B. Averyt, M. Tignor and H.L. Miller (eds.)], Cambridge University Press, Cambridge, United Kingdom and New York, NY, USA.

Barnston, A. G., and Livezey, R. E. 1987. Classification, seasonality and persistence of low-frequency atmospheric circulation patterns. Mon. Wea. Rev., 115, 1083-1126.

Brickman, D., Wang, Z., and Detracy, B. 2016. Variability of Current Streams in Atlantic Canadian Waters: A Model Study. Atmosphere-Ocean, 54:3, 218-229, DOI: 10.1080/07055900.2015.1094026

Brickman, D., Hebert, D., and Wang, Z. 2018. Mechanism for the recent ocean warming events on the Scotian Shelf of eastern Canada. Cont. Shelf Res. 156, 11-22 https://doi.org/10.1016/j.csr.2018.01.001.

Cavalieri, D. J., Parkinson, C.L., Gloersen, P., and Zwally, H.J. 1996. updated yearly. *Sea Ice Concentrations from Nimbus-7 SMMR and DMSP SSM/I-SSMIS Passive Microwave Data, Version 1*. [north/monthly]. Boulder, Colorado USA. NASA National Snow and Ice Data Center Distributed Active Archive Center. doi: https://doi.org/10.5067/8GQ8LZQVL0VL. [Accessed 05/12/2018].

Curry, R., R.R. Dickson, and I. Yashayaev, 2003, A change in the freshwater balance of the Atlantic Ocean over the past four decades, Nature, 426, 826 – 829.

Dickson, R.R., I. Yashayaev, J. Meincke, W.R. Turrell, S.R. Dye, and J. Holfort, 2002. Rapid freshening of the deep North Atlantic Ocean over the past four decades. Nature, 416, 832–837.

Dukhovskoy D. S., I. Yashayaev, A. Proshutinsky, J. L. Bamber, I. L. Bashmachnikov, E. P. Chassignet, C. M. Lee and A. J. Tedstone, 2019, Role of Greenland Freshwater Anomaly in the Recent Freshening of the Subpolar North Atlantic, Journal of Geophysical Research: Oceans, Volume 124, Issue 5, Pages 3333-3360, https://doi.org/10.1029/2018JC014686.

Fetterer, F., Knowles, K., Meier, W. and Savoie, M. 2002. Updated 2011. Sea ice index. Boulder, CO: National Snow and Ice Data Center. Digital media.

Fragoso, G.M., Poulton, A.J., Yashayaev, I., Head, E.J.H., Stinchcombe, M., and Purdie, D.A. 2016. Biogeographical patterns and environmental controls of phytoplankton communities from contrasting hydrographical zones of the Labrador Sea, Progress in Oceanography, V.141, 212–226.

Fröb, F., Olsen, A., Våge, K., Moore, K., Yashayaev, I., Jeansson, E., and Rajasakaren, B. 2016. Irminger Sea deep convection injects oxygen and anthropogenic carbon to the ocean interior, Nature Communications, 13244, doi: 10.1038/ncomms13244.

Hauser, T., Demirov, E., Zhu, J., and Yashayaev, I. 2015. North Atlantic atmospheric and ocean inter-annual variability over the past fifty years – Dominant patterns and decadal shifts. Progress in Oceanography, Volume 132, March 2015, Pages 197–219.

Holliday, N.P., Bersch, M., Berx, B. et al. Ocean circulation causes the largest freshening event for 120 years in eastern subpolar North Atlantic. Nature Communications 11, 585 (2020). https://doi.org/10.1038/s41467-020-14474-y.

Hurrell, J.W. 1995. Decadal trends in the North Atlantic Oscillation: Regional temperatures and precipitation. Science, 269, 676-679.

Hurrell, J. W. and National Center for Atmospheric Research Staff Eds. (Last modified 04 Aug 2018), "The Climate Data Guide: Hurrell North Atlantic Oscillation (NAO) Index (station-based)." Retrieved from https://climatedataguide.ucar.edu/climate-data/hurrell-north-atlantic-oscillation-nao-index-station-based.

Kalnay, E., Kanamitsu, M., Kistler, R., Collins, W., Deaven, D., Gandin, L., Iredell, M., Saha, S., White, G., Woollen, J., Zhu, Y., Chelliah, M., Ebisuzaki, W., Higgins, W., Janowiak, J., Mo, K.C., Ropelewski, C., Wang, J., Leetmaa, A., Reynolds, R., Jenne, R., and Joseph, D. 1996. The NCEP/NCAR 40-Year Reanalysis Project., Bull. Amer. Meteor. Soc., 77, No. 3, 437-470.

Kieke, D., and Yashayaev, I. 2015. Studies of Labrador Sea Water formation and variability in the subpolar North Atlantic in the light of international partnership and collaboration, Progress in Oceanography, doi:10.1016/j.pocean.2014.12.010.

Lazier, J. R. N., Hendry, R. M., Clarke, R. A., Yashayaev, I., and Rhines, P. 2002. Convection and restratification in the Labrador Sea, 1990– 2000, Deep Sea Res., Part A, 49, 1819– 1835. https://doi.org/10.1016/S0967-0637(02)00064-X

Lozier, M.S., et al., 2019. A sea change in our view of overturning in the subpolar North Atlantic, Science, Vol. 363, Issue 6426, pp. 516-521, DOI: 10.1126/science.aau6592.

Meier, W. N., Fetterer, F., and Windnagel, A. K. 2017. *Near-Real-Time NOAA/NSIDC Climate Data Record of Passive Microwave Sea Ice Concentration, Version 1*. [north/daily]. doi: https://doi.org/10.7265/N5FF3QJ6. [Accessed 05/12/2018].

Progress in Oceanography, 2007, Observing and Modelling Ocean Heat and Freshwater Budgets and Transports, Edited by Igor Yashayaev, Vol. 73, 3-4, May-June 2007, Pages 203-426.

Progress in Oceanography, 2015, Oceanography of the Arctic and North Atlantic Basins, Edited by Igor Yashayaev, Dan Seidov, Entcho Demirov, Vol. 132, March 2015, Pages 1-352.

Rhein, M., S.R. Rintoul, S. Aoki, E. Campos, D. Chambers, R.A. Feely, S. Gulev, G.C. Johnson, S.A. Josey, A. Kostianoy, C. Mauritzen, D. Roemmich, L.D. Talley and F. Wang. 2013. Observations: Ocean. In: Climate Change 2013: The Physical Science Basis. Contribution of Working Group I to the Fifth Assessment Report of the Intergovernmental Panel on Climate Change [Stocker, T.F., D. Qin, G.-K. Plattner, M. Tignor, S.K. Allen, J. Boschung, A. Nauels, Y. Xia, V. Bex and P.M. Midgley (eds.)]. Cambridge University Press, Cambridge, United Kingdom and New York, NY, USA.

Smeed, D. A., Josey, S. A., Beaulieu, C., Johns, W. E., Moat, B. I., Frajka-Williams, E., et al. 2018. The North Atlantic Ocean is in a state of reduced overturning. Geophysical Research Letters, 45, 1527–1533. https://doi.org/10.1002/2017GL076350

Thornalley, D.J.R., Oppo, D.W., Ortega, P., Robson, J.I., Brierley, C.M., Davis, R., Hall, I.R., Moffa-Sanchez, P., Rose, N.L., Spooner, P.T., Yashayaev, I., Keigwin., L.D. 2018, Anomalously weak Labrador Sea convection and Atlantic overturning during the past 150 years. Nature, 2018; 556 (7700): 227 DOI: 10.1038/s41586-018-0007-4

Visbeck, M.H., Hurrell, J.W., Polvani, L., and Cullen, H.M. 2001. The North Atlantic Oscillation: Past, Present and Future. Proc. Nat. Acad. Sci., 98, 12876-12877 doi: 10.1073/pnas.231391598.

Wang, Z., Brickman, D., Greenan, B., and Yashayaev, I. 2016. An abrupt shift in the Labrador Current System in relation to winter NAO events. Journal of Geophysical Research: Oceans. DOI: 10.1002/2016JC011721.

Wang, Z., Lu, Y., Greenan, B., Brickman, D., and DeTracey, B. 2018. BNAM: An eddy-resolving North Atlantic Ocean model to support ocean monitoring. Can. Tech. Rep. Hydrogr. Ocean. Sci. 327: vii + 18p.

Wang, Z., D. Brickman, and B. Greenan, 2019. Characteristic evolution of the Atlantic Meridional Overturning Circulation from 1990 to 2015: An eddy-resolving ocean model study. Deep Sea Research Part I, https://doi.org/10.1016/j.dsr.2019.06.002.

Yashayaev, I. 2007. Hydrographic changes in the Labrador Sea, 1960-2005, Progress in Oceanography, 73, 242-276.

Yashayaev, I., and Dickson, R. R. 2008. Chapter 21. Transformation and Fate of Overflows in the northern North Atlantic, Arctic-Subarctic Ocean Fluxes: Defining the Role of the Northern Seas in Climate, R.R.Dickson, J.Meincke, P.Rhines (Eds.), Springer (www.springer.com), ISBN: 978-1-4020-6773-0.

Yashayaev, I., and Loder, J.W. 2009. Enhanced production of Labrador Sea Water in 2008. Geophys. Res. Lett., 36: L01606, doi:10.1029/2008GL036162.

Yashayaev, I., Seidov, D., and Demirov, E. 2015. A new collective view of oceanography of the Arctic and North Atlantic basins, Progress in Oceanography, doi:10.1016/j.pocean.2014.12.012.

Yashayaev, I., and Seidov, D. 2015. The role of the Atlantic Water in multidecadal ocean variability in the Nordic and Barents Seas, Progress in Oceanography, doi:10.1016/j.pocean.2014.11.009.

Yashayaev, I., and Loder, J.W. 2016. Recurrent replenishment of Labrador Sea Water and associated decadal-scale variability. Journal of Geophys. Res.: Oceans, 121, 11, DOI: 10.1002/2016JC012046.

Yashayaev, I., and Loder, J.W. 2017. Further intensification of deep convection in the Labrador Sea in 2016. Geophysical Research Letters, 44, 3, DOI: 10.1002/2016GL071668.